Journal of Scientific Computing (2024) 101:48
https://doi.org/10.1007/s10915-024-02690-3

Convergence Analysis of an Implicit Finite Difference Method for the Inertial Landau–Lifshitz–Gilbert Equation

Jingrun Chen[1,2] · Panchi Li[3] · Cheng Wang[4]

Received: 6 September 2022 / Revised: 4 August 2024 / Accepted: 29 September 2024 /
Published online: 8 October 2024

Abstract

The Landau–Lifshitz–Gilbert (LLG) equation is widely used to model the fast magnetization dynamics of ferromagnets. Recent experimental observations have revealed ultra-fast dynamics at the sub-picosecond timescale, and the inertial LLG equation is proposed to capture the ultra-fast behaviour of magnetization, in which a second temporal derivative of magnetization (inertial term) is introduced. The inertial LLG equation is therefore a mixed hyperbolic-parabolic type equation with degeneracy, which produces extra difficulties in numerical analysis. In this paper, we propose an implicit finite difference scheme based on the central difference in both time and space, and a fixed point iteration method to solve the nonlinear system. By a constructed solution with second order accuracy, we get a linear system and provide an unconditional convergence analysis in $\ell^\infty([0, T]; H_h^1(\Omega))$.. We demonstrate that the proposed method is second order accurate in both time and space, a natural preservation of the magnetization length and the energy decaying. In the hyperbolic regime, significant nutation of magnetization at a shorter timescale are simulated by numerical simulations.

Keywords Convergence analysis · Inertial Landau–Lifshitz–Gilbert equation · Implicit central difference scheme · Second order accuracy

Mathematics Subject Classification 35K61 · 65M06 · 65M12

✉ Panchi Li
LiPanchi1994@163.com

Jingrun Chen
jingrunchen@ustc.edu.cn

Cheng Wang
cwang1@umassd.edu

1 School of Mathematical Sciences, University of Science and Technology of China, Hefei 230026, Anhui, China

2 Suzhou Institute for Advanced Research, University of Science and Technology of China, Suzhou 215123, Jiangsu, China

3 School of Mathematical Sciences, Soochow University, Suzhou 215006, China

4 Mathematics Department, University of Massachusetts, North Dartmouth, MA 02747, USA

1 Introduction

The Landau–Lifshitz–Gilbert (LLG) equation [17, 22] describes the dissipative magnetization dynamics in ferromagnetic materials. It is widely used to interpret the experimental observations and study the magnetization dynamics. However, recent experiments [6, 18, 19] confirm that its validity is limited to timescales from picosecond to larger timescales for which the angular momentum reaches equilibrium in a force field. At shorter timescales, e.g. ~ 100 fs, the ultra-fast magnetization dynamics would exhibit [19], which can be modeled by the inertial Landau–Lifshitz–Gilbert (iLLG) equation [7, 13, 15]. When the inertial effect is activated by a non-equilibrium initialization or an external magnetic field, the magnetization converges to its equilibrium along a locus with a damping nutation [24].

For a ferromagnet over $\Omega \subset \mathbb{R}^d$, $d = 1, 2, 3$, the observable states are depicted by the distribution of the magnetization in Ω, in which the magnetization denoted by $\boldsymbol{m}(\boldsymbol{x}, t)$ is a vector field taking values on the unit sphere $\mathbb{S}^2$. From a given initialization of magnetization configuration, the system reaches one of local minimal of the corresponding magnetic free energy functional under the guidance of the LLG equation with an effective field. The dynamic evolution of the system, also referred as the stabilization and transition of these magnetic states, is crucial to the applications of ferromagnetic materials. To understand and exploit the complex mechanism, micromagnetics simulations have become increasingly important over the past several decades, in addition to experiment observations and theoretical predications.

One of the core problems in micromagnetics simulations is to find the numerical solution of the LLG equation. In the past decades, various numerical approaches have been proposed; see [12, 21] for reviews and references therein. In terms of the time marching approach, the simplest explicit algorithms, such as the forward Euler method and Runge-Kutta methods, were favored in the early days, while small time step size must be adopted due to the stability restriction [25]. Implicit methods can avoid the stability constraint,while a step-size condition $k = O(h^2)$ is usually required in both the theoretical analysis and numerical simulations [2, 3]. Implicit methods also suffer from the low efficiency since iteration methods are commonly necessary. To obtain the numerical solution with high-efficiency, various of semi-implicit methods have been proposed in recent years, such as the Gauss-Seidel projection methods [14, 23, 29], the linearized backward Euler scheme [11, 16], the Crank-Nicolson projection scheme [4], and the second order semi-implicit backward differentiation formula projection scheme [8–10, 30]. In practice, all these semi-implicit methods inherit the unconditional stability of implicit schemes, and achieve a considerable improvement in efficiency. Furthermore, an alternative class of time integration methods has been proposed within the finite element framework [1], such as the first-order tangent plane scheme (TPS) and the second-order angular momentum method (AMM) [20]. By defining an intermediate variable $\boldsymbol{v} = \partial_t \boldsymbol{m}$, this class of numerical method solves $\boldsymbol{v}$ in the tangent space of $\boldsymbol{m}$, followed by a projection step to obtain the numerical solution. An unconditional stable TPS solves a linear equation with variable coefficients at each time step, while a nonlinear equation must be solved in the AMM approach. Henceforth, the efficiency of the TPS and AMM are proportional with the semi-implicit methods.

The LLG equation is a nonlinear parabolic system which consists of the gyromagnetic term and the damping term. It is a classical kinetic equation that solely incorporates velocity, with no consideration given to acceleration. When relaxing the system from a non-equilibrium state or applying a perturbation, it is reasonable to expect the presence of an acceleration term. Consequently, this leads to an inertial term within the iLLG equation. More specifically, the time evolution of $\boldsymbol{m}(\boldsymbol{x}, t)$ is described by $\partial_t \boldsymbol{m}$, and an inertial term $\boldsymbol{m} \times \partial_{tt} \boldsymbol{m}$ is added to the term $\boldsymbol{m} \times \partial_t \boldsymbol{m}$. Therefore, the iLLG equation is a nonlinear system of mixed hyperbolic-parabolic type with degeneracy. The TPS and AMM are firstly proposed to study the nutation of iLLG equation, and these two methods aim to find a weak solution. Meanwhile, based on the finite difference spatial approximation, a second-order accurate semi-implicit method is presented in [24], and $\partial_{tt}\boldsymbol{m}$ and $\partial_t \boldsymbol{m}$ are approximated by the central difference discretization.

In this work, we provide the convergence analysis of the implicit mid-point scheme on three time layers for the iLLG equation. The unique solvability is subjected to the condition $k \le Ch^2$. Nevertheless, by an introduced approximation solution, we construct a linear problem for the error estimate, and thus we can obtain its unconditional convergence in $H^1(\Omega_T)$. Owing to the application of the mid-point scheme, the proposed method naturally preserves the magnetization length. Moreover, we propose a fixed-point iteration method to solve the nonlinear scheme, which converges to a unique solution under the condition of $k \le Ch^2$. Numerical simulations are reported to confirm the theoretic analysis, and the inertial dynamics at shorter timescales is studied.

The rest of this paper is organized as follows. The iLLG equation and the numerical method are introduced in Sect. 2. The detailed convergence analysis is provided in Sect. 3. In addition, a fixed-point iteration method for solving the implicit scheme is proposed in Sect. 4, and the convergence is established upon the condition $k \le Ch^2$. Numerical tests, including the accuracy test and observation of the inertial effect, are presented in Sect. 5. Concluding remarks are made in Sect. 6.

2 The Physical Model and the Numerical Method

The intrinsic magnetization of a ferromagnet $\boldsymbol{m} = \boldsymbol{m}(\boldsymbol{x}, t) : \Omega_T := \Omega \times (0, T) \to \mathbb{S}^2$ is modeled by the conventional LLG equation:

$$\partial_t \boldsymbol{m} = -\boldsymbol{m} \times \Delta \boldsymbol{m} + \alpha \boldsymbol{m} \times \partial_t \boldsymbol{m}, \qquad (\boldsymbol{x}, t) \in \Omega_T, \tag{2.1a}$$

$$\boldsymbol{m}(\boldsymbol{x}, 0) = \boldsymbol{m}(0), \qquad \boldsymbol{x} \in \Omega, \tag{2.1b}$$

$$\partial_\nu \boldsymbol{m}(\boldsymbol{x}, t) = 0, \qquad (\boldsymbol{x}, t) \in \partial\Omega \times [0, T], \tag{2.1c}$$

where ν represents the unit outward normal vector on $\partial\Omega$, and $\alpha \ll 1$ is the damping parameter. When the relaxation starts from a non-equilibrium state or a perturbation is applied, the acceleration would be present in the kinetic equation, which is the inertial effect observed in various experiments at the sub-picosecond timescale. In turn, its dynamics is described by the iLLG equation

$$\partial_t \boldsymbol{m} = -\boldsymbol{m} \times (\Delta \boldsymbol{m} + \mathbf{H}_\mathrm{e}) + \alpha \boldsymbol{m} \times (\partial_t \boldsymbol{m} + \tau \partial_{tt} \boldsymbol{m}), \qquad (\boldsymbol{x}, t) \in \Omega_T, \tag{2.2a}$$

$$\boldsymbol{m}(\boldsymbol{x}, 0) = \boldsymbol{m}(0), \qquad \boldsymbol{x} \in \Omega, \tag{2.2b}$$

$$\partial_t \boldsymbol{m}(\boldsymbol{x}, 0) = 0, \qquad \boldsymbol{x} \in \Omega, \tag{2.2c}$$

$$\partial_\nu \boldsymbol{m}(\boldsymbol{x}, t) = 0, \qquad (\boldsymbol{x}, t) \in \partial\Omega \times [0, T], \tag{2.2d}$$

where τ is the phenomenological inertia parameter, and $\mathbf{H}_\mathrm{e}$ is a perturbation of the external magnetic field. To ease the discussion, the external field is neglected in the subsequent analysis and only considered in micromagnetics simulations. Here the additional initial condition $\partial_t \boldsymbol{m}(\boldsymbol{x}, 0) = 0$ is added, which implies that the velocity is 0 at $t = 0$ and it is a necessary condition for the well-posedness. Then the magnetic energy functional is

$$\mathcal{E}[\boldsymbol{m}] = \frac{1}{2} \int_\Omega \left(|\nabla \boldsymbol{m}|^2 - 2\boldsymbol{m} \cdot \mathbf{H}_\mathrm{e} + \alpha\tau \, |\partial_t \boldsymbol{m}|^2 \right) \mathrm{d}\boldsymbol{x}. \tag{2.3}$$

For constant external magnetic fields, it satisfies the energy dissipation law

$$\frac{d}{dt}\mathcal{E}[\boldsymbol{m}] = -\alpha \int_{\Omega} |\partial_t \boldsymbol{m}|^2 \mathrm{d}\boldsymbol{x} \leq 0. \tag{2.4}$$

Therefore, under the condition of (2.2c), for almost all $T' \in [0, T]$, we have

$$\frac{1}{2}\int_{\Omega} \left(|\nabla \boldsymbol{m}(\boldsymbol{x}, T')|^2 + \alpha\tau \left|\partial_t \boldsymbol{m}(\boldsymbol{x}, T')\right|^2 \right) \mathrm{d}\boldsymbol{x} \leq \frac{1}{2}\int_{\Omega} \left(|\nabla \boldsymbol{m}(\boldsymbol{x}, 0)|^2 \right) \mathrm{d}\boldsymbol{x}. \tag{2.5}$$

Before the formal algorithm is presented, here the spatial difference mesh and the temporal discretization is stated. We consider the uniform mesh for Ω with mesh-size h and a time step-size $k > 0$. Let L be the set of nodes $\{\boldsymbol{x}_l = (x_i, y_j, z_k)\}$ in 3-D space with the indices $i = 0, 1, \cdots, nx, nx+1$, $j = 0, 1, \cdots, ny, ny+1$ and $k = 0, 1, \cdots, nz, nz+1$, in which ghost points on the boundary $\partial\Omega$ are denoted by $i = 0, nx+1$, $j = 0, ny+1$ and $k = 0, nz+1$. We use the half grid points with $\boldsymbol{m}_{i,j,k} = \boldsymbol{m}((i-\frac{1}{2})h, (j-\frac{1}{2})h, (k-\frac{1}{2})h)$. Due to the homogeneous Neumann boundary condition (2.2d), the following extrapolation formula is derived:

$$\boldsymbol{m}_{i_x+1,j,k} = \boldsymbol{m}_{i_x,j,k}, \boldsymbol{m}_{i,j_y+1,k} = \boldsymbol{m}_{i,j_y,k}, \boldsymbol{m}_{i,j,k_z+1} = \boldsymbol{m}_{i,j,k_z} \tag{2.6}$$

for all $1 \leq i \leq nx$, $1 \leq j \leq ny$, $1 \leq k \leq nz$, where $i_x = 0, nx$, $j_y = 0, ny$ and $k_z = 0, nz$.

Meanwhile, for the time stepping, we define the difference formulates as follows.

Definition 1 For $\phi^{n+1} = \phi(\boldsymbol{x}, t_{n+1})$ and $\psi^{n+1} = \psi(t_{n+1})$, define

$$d_t^+ \phi^n = \frac{\phi^{n+1} - \phi^n}{k}, \quad d_t^- \phi^n = \frac{\phi^n - \phi^{n-1}}{k},$$

and

$$D_t^+ \psi^n = \frac{\psi^{n+1} - \psi^n}{k}, \quad D_t^- \psi^n = \frac{\psi^n - \psi^{n-1}}{k}.$$

Consequently, we denote

$$d_t \phi^{n+1} = \frac{1}{2}(d_t^+ \phi^n + d_t^- \phi^n), \quad D_t \psi^{n+1} = \frac{1}{2}(D_t^+ \psi^n + D_t^- \psi^n).$$

In particular, the second time derivative is approximated by the central difference form

$$d_{tt}\phi = \frac{\phi^{n+1} - 2\phi^n + \phi^{n-1}}{k^2}. \tag{2.7}$$

Then for the initial condition (2.2c), there holds

$$\boldsymbol{m}(\boldsymbol{x}_l, 0) = \boldsymbol{m}(\boldsymbol{x}_l, k), \ \forall l \in L, \tag{2.8}$$

on the mesh grid. Given grid functions $\boldsymbol{f}_h, \boldsymbol{g}_h \in \ell^2(\Omega_h, \mathbb{R}^3)$, we list definitions of the discrete inner product and norms used in this paper.

Definition 2 The discrete inner product $\langle \cdot, \cdot \rangle$ in $\ell^2(\Omega_h, \mathbb{R}^3)$ is defined by

$$\langle \boldsymbol{f}_h, \boldsymbol{g}_h \rangle = h^d \sum_{l \in L} \boldsymbol{f}_h(\boldsymbol{x}_l) \cdot \boldsymbol{g}_h(\boldsymbol{x}_l). \tag{2.9}$$

The discrete ℓ^2 norm and H_h^1 norm of $\boldsymbol{m}_h$ are

$$\|\boldsymbol{f}_h\|_2^2 = h^d \sum_{l \in L} \boldsymbol{f}_h(\boldsymbol{x}_l) \cdot \boldsymbol{f}_h(\boldsymbol{x}_l), \tag{2.10}$$

and

$$\|\boldsymbol{f}_h\|_{H_h^1}^2 = \|\boldsymbol{f}_h\|_2^2 + \|\nabla_h \boldsymbol{f}_h\|_2^2 \tag{2.11}$$

with ∇_h representing the central difference stencil of the gradient operator.

Besides, the norm $\|\cdot\|_\infty$ in $\ell^\infty(\Omega_h, \mathbb{R}^3)$ is defined by

$$\|\boldsymbol{f}_h\|_\infty = \max_{l\in L} \|\boldsymbol{f}_h(\boldsymbol{x}_l)\|_\infty. \tag{2.12}$$

Denote $\boldsymbol{m}_h^n (n \geq 0)$ as the numerical solution, and the approximation scheme of the iLLG equation is presented below.

Algorithm 1 *Given $\boldsymbol{m}_h^0, \boldsymbol{m}_h^1 \in W^{1,2}(\Omega_h, \mathbb{S}^2)$. Let $\boldsymbol{m}_h^{n-1}, \boldsymbol{m}_h^n \in W^{1,2}(\Omega_h, \mathbb{S}^2)$, we compute $\boldsymbol{m}_h^{n+1}$ by*

$$d_t\boldsymbol{m}_h^{n+1} - \alpha\bar{\boldsymbol{m}}_h^n \times \left(d_t\boldsymbol{m}_h^{n+1} + \tau d_{tt}\boldsymbol{m}_h^n\right) = -\bar{\boldsymbol{m}}_h^n \times \Delta_h\bar{\boldsymbol{m}}_h^n, \tag{2.13}$$

where $\bar{\boldsymbol{m}}_h^n = \frac{1}{2}(\boldsymbol{m}_h^{n+1} + \boldsymbol{m}_h^{n-1})$, and Δ_h represents the standard seven-point stencil of the Laplacian operator.

The corresponding fully discrete version of the above (2.13) reads as

$$\begin{aligned}&\frac{\boldsymbol{m}_h^{n+1} - \boldsymbol{m}_h^{n-1}}{2k} - \alpha\frac{\boldsymbol{m}_h^{n+1} + \boldsymbol{m}_h^{n-1}}{2} \times \left(\frac{\boldsymbol{m}_h^{n+1} - \boldsymbol{m}_h^{n-1}}{2k} + \tau\frac{\boldsymbol{m}_h^{n+1} - 2\boldsymbol{m}_h^n + \boldsymbol{m}_h^{n-1}}{k^2}\right)\\ &= -\frac{\boldsymbol{m}_h^{n+1} + \boldsymbol{m}_h^{n-1}}{2} \times \Delta_h\left(\frac{\boldsymbol{m}_h^{n+1} + \boldsymbol{m}_h^{n-1}}{2}\right).\end{aligned} \tag{2.14}$$

The second-order spatial and temporal approximation can be directly obtained by the Taylor expansion:

$$\begin{aligned}&\frac{\boldsymbol{m}(\boldsymbol{x}_l, t_{n+1}) - 2\boldsymbol{m}(\boldsymbol{x}_l, t_n) + \boldsymbol{m}(\boldsymbol{x}_l, t_{n-1})}{k^2}\\ &= \partial_{tt}\boldsymbol{m}(\boldsymbol{x}_l, t_n) + \frac{k^2}{12}\partial_t^{(4)}\boldsymbol{m}(\boldsymbol{x}_l, t_n) + \cdots,\end{aligned} \tag{2.15}$$

and

$$\begin{aligned}\Delta_h\left(\frac{\boldsymbol{m}(\boldsymbol{x}_l, t_{n+1}) + \boldsymbol{m}(\boldsymbol{x}_l, t_{n-1})}{2}\right) &= \Delta_h\boldsymbol{m}(\boldsymbol{x}_l, t_n) + \frac{k^2}{2}\Delta_h\partial_{tt}\boldsymbol{m}(\boldsymbol{x}_l, t_n) + \cdots\\ &= \Delta\boldsymbol{m}(\boldsymbol{x}_l, t_n) + \frac{h^2}{12}\Delta^2\boldsymbol{m}(\boldsymbol{x}_l, t_n) + \frac{k^2}{2}\Delta\partial_{tt}\boldsymbol{m}(\boldsymbol{x}_l, t_n) + \cdots.\end{aligned} \tag{2.16}$$

The two expansions indicate a regularity requirement for the classical solution $\boldsymbol{m}$, in the space $C^4([0, T]; [C^0(\bar{\Omega})]^3) \cap C^2([0, T]; [C^2(\bar{\Omega})]^3) \cap L^\infty([0, T]; [C^4(\bar{\Omega})]^3)$.

Due to the mid-point approximation feature, this implicit scheme is excellent in maintaining certain properties of the original system.

Lemma 1 *Given $\left|\boldsymbol{m}_h^0(\boldsymbol{x}_l)\right| = 1$, then the sequence $\{\boldsymbol{m}_h^n(\boldsymbol{x}_l)\}_{n\geq 0}$ produced by (2.13) satisfies*

(i) $\left|\boldsymbol{m}_h^n(\boldsymbol{x}_l)\right| = 1, \forall l \in L;$
(ii) $\frac{1}{2}D_t\|\nabla_h\boldsymbol{m}_h^{n+1}\|_2^2 + \alpha\|d_t\boldsymbol{m}_h^{n+1}\|_2^2 + \frac{1}{2}\alpha\tau D_t^-\|d_t^+\boldsymbol{m}_h^n\|_2^2 = 0.$

Proof Employing the (2.2c) firstly yields $\boldsymbol{m}^0(\boldsymbol{x}_l) = \boldsymbol{m}^1(\boldsymbol{x}_l)$ for all $l \in L$. Take the vector inner product with (2.13) by $(\boldsymbol{m}_h^{n+1}(\boldsymbol{x}_l) + \boldsymbol{m}_h^{n-1}(x_l))$, and we get

$$|\boldsymbol{m}_h^{n+1}| = |\boldsymbol{m}_h^n| = \cdots = |\boldsymbol{m}_h^1| = |\boldsymbol{m}_h^0| = 1,$$

in the point-wise sense. This confirms (i). In order to verify (ii), we take inner product with (2.13) by $-\Delta_h \bar{\boldsymbol{m}}_h^n$ and get

$$\frac{1}{2} D_t \|\nabla_h \boldsymbol{m}_h^{n+1}\|_2^2 - \alpha \langle \bar{\boldsymbol{m}}_h^n \times d_t \boldsymbol{m}_h^{n+1}, -\Delta_h \bar{\boldsymbol{m}}_h^n \rangle - \alpha\tau \langle \boldsymbol{m}_h^n \times d_{tt} \boldsymbol{m}_h^n, -\Delta_h \bar{\boldsymbol{m}}_h^n \rangle = 0.$$

Subsequently, taking inner products with $d_t \boldsymbol{m}_h^{n+1}$ and $d_{tt} \boldsymbol{m}_h^{n+1}$ separately leads to the following equalities:

$$\|d_t \boldsymbol{m}_h^{n+1}\|_2^2 - \alpha\tau \langle \boldsymbol{m}_h^n \times d_{tt} \boldsymbol{m}_h^n, d_t \boldsymbol{m}_h^{n+1} \rangle = -\langle \bar{\boldsymbol{m}}_h^n \times d_t \boldsymbol{m}_h^{n+1}, -\Delta_h \bar{\boldsymbol{m}}_h^n \rangle,$$

and

$$\frac{1}{2} D_t^- \|d_t^+ \boldsymbol{m}_h^n\|_2^2 + \alpha \langle \boldsymbol{m}_h^n \times d_{tt} \boldsymbol{m}_h^n, d_t \boldsymbol{m}_h^{n+1} \rangle = -\langle \boldsymbol{m}_h^n \times d_{tt} \boldsymbol{m}_h^n, -\Delta_h \bar{\boldsymbol{m}}_h^n \rangle.$$

A combination of the above three identities yields (ii).

In Lemma 1, taking $k \to 0$ gives

$$\frac{\mathrm{d}}{\mathrm{d}t} \left(\frac{1}{2} \|\nabla_h \boldsymbol{m}_h^{n+1}\|_2^2 + \frac{\alpha\tau}{2} \|\partial_t \boldsymbol{m}_h^n\|_2^2 \right) = -\alpha \|\partial_t \boldsymbol{m}_h^{n+1}\|_2^2, \tag{2.17}$$

which is consistent with the continuous energy law (2.4). Accordingly, in the absence of the external magnetic field, the discretized version energy dissipation law is maintained with a modification

$$E(\boldsymbol{m}_h^{n+1}, \boldsymbol{m}_h^n) = \frac{\alpha\tau}{2} \left\| \frac{\boldsymbol{m}_h^{n+1} - \boldsymbol{m}_h^n}{k} \right\|_2^2 + \frac{1}{4} (\|\nabla_h \boldsymbol{m}_h^{n+1}\|_2^2 + \|\nabla_h \boldsymbol{m}_h^n\|_2^2). \tag{2.18}$$

Theorem 1 *Given $\boldsymbol{m}_h^{n-1}, \boldsymbol{m}_h^n, \boldsymbol{m}_h^{n+1} \in W^{1,2}(\Omega_h, \mathbb{S}^2)$, we have a discrete energy dissipation law, for the modified energy (2.18):*

$$E(\boldsymbol{m}_h^{n+1}, \boldsymbol{m}_h^n) \le E(\boldsymbol{m}_h^n, \boldsymbol{m}_h^{n-1}). \tag{2.19}$$

Proof Denote a discrete function

$$\mu^n := \alpha \Big(\frac{\boldsymbol{m}_h^{n+1} - \boldsymbol{m}_h^{n-1}}{2k} + \tau \frac{\boldsymbol{m}_h^{n+1} - 2\boldsymbol{m}_h^n + \boldsymbol{m}_h^{n-1}}{k^2} \Big) - \frac{1}{2} \Delta_h (\boldsymbol{m}_h^{n+1} + \boldsymbol{m}_h^{n-1}).$$

Taking a discrete inner product with (2.13) by μ^n gives

$$\begin{aligned} &\frac{\alpha}{4k^2} \langle \boldsymbol{m}_h^{n+1} - \boldsymbol{m}_h^{n-1}, \boldsymbol{m}_h^{n+1} - \boldsymbol{m}_h^{n-1} \rangle + \frac{\alpha\tau}{2k^3} \langle \boldsymbol{m}_h^{n+1} - \boldsymbol{m}_h^{n-1}, \boldsymbol{m}_h^{n+1} - 2\boldsymbol{m}_h^n + \boldsymbol{m}_h^{n-1} \rangle \\ &\quad + \frac{\alpha}{4k} \Big\langle \boldsymbol{m}_h^{n+1} - \boldsymbol{m}_h^{n-1}, -\Delta_h (\boldsymbol{m}_h^{n+1} + \boldsymbol{m}_h^{n-1}) \Big\rangle \\ &\quad = \Big\langle - \frac{\boldsymbol{m}_h^{n+1} + \boldsymbol{m}_h^{n-1}}{2} \times \mu^n, \mu^n \Big\rangle = 0. \end{aligned} \tag{2.20}$$

Meanwhile, the following estimates are available:

$$\begin{aligned} &\langle \boldsymbol{m}_h^{n+1} - \boldsymbol{m}_h^{n-1}, \boldsymbol{m}_h^{n+1} - \boldsymbol{m}_h^{n-1} \rangle = \|\boldsymbol{m}_h^{n+1} - \boldsymbol{m}_h^{n-1}\|_2^2 \ge 0, \\ &\langle \boldsymbol{m}_h^{n+1} - \boldsymbol{m}_h^{n-1}, \boldsymbol{m}_h^{n+1} - 2\boldsymbol{m}_h^n + \boldsymbol{m}_h^{n-1} \rangle \end{aligned}$$

$$
\begin{aligned}
&= \Big\langle (\boldsymbol{m}_h^{n+1} - \boldsymbol{m}_h^n) + (\boldsymbol{m}_h^n - \boldsymbol{m}_h^{n-1}), (\boldsymbol{m}_h^{n+1} - \boldsymbol{m}_h^n) - (\boldsymbol{m}_h^n - \boldsymbol{m}_h^{n-1}) \Big\rangle, \qquad (2.21)\\
&= \|\boldsymbol{m}_h^{n+1} - \boldsymbol{m}_h^n\|_2^2 - \|\boldsymbol{m}_h^n - \boldsymbol{m}_h^{n-1}\|_2^2,\\
&\Big\langle \boldsymbol{m}_h^{n+1} - \boldsymbol{m}_h^{n-1}, -\Delta_h(\boldsymbol{m}_h^{n+1} + \boldsymbol{m}_h^{n-1}) \Big\rangle\\
&= \Big\langle \nabla_h(\boldsymbol{m}_h^{n+1} - \boldsymbol{m}_h^{n-1}), \nabla_h(\boldsymbol{m}_h^{n+1} + \boldsymbol{m}_h^{n-1}) \Big\rangle = \|\nabla_h \boldsymbol{m}_h^{n+1}\|_2^2 - \|\nabla_h \boldsymbol{m}_h^{n-1}\|_2^2 \qquad (2.22)\\
&= (\|\nabla_h \boldsymbol{m}_h^{n+1}\|_2^2 + \|\nabla_h \boldsymbol{m}_h^n\|_2^2) - (\|\nabla_h \boldsymbol{m}_h^n\|_2^2 + \|\nabla_h \boldsymbol{m}_h^{n-1}\|_2^2). \qquad (2.23)
\end{aligned}
$$

Going back to (2.20), we arrive at

$$
\begin{aligned}
&\frac{\alpha\tau}{2k}\Big(\Big\| \frac{\boldsymbol{m}_h^{n+1} - \boldsymbol{m}_h^n}{k} \Big\|_2^2 - \Big\| \frac{\boldsymbol{m}_h^n - \boldsymbol{m}_h^{n-1}}{k} \Big\|_2^2 \Big)\\
&\quad + \frac{1}{4k}\Big((\|\nabla_h \boldsymbol{m}_h^{n+1}\|_2^2 + \|\nabla_h \boldsymbol{m}_h^n\|_2^2) - (\|\nabla_h \boldsymbol{m}_h^n\|_2^2 + \|\nabla_h \boldsymbol{m}_h^{n-1}\|_2^2) \Big)\\
&\quad = -\alpha \Big\| \frac{\boldsymbol{m}_h^{n+1} - \boldsymbol{m}_h^{n-1}}{2k} \Big\|_2^2 \le 0, \qquad (2.24)
\end{aligned}
$$

which is exactly the energy dissipation estimate (2.19). This finishes the proof of Theorem 1. □

On the other hand, due to its nonlinearity, the unique solvability is ensured by a constraint $k \le Ch^2$, with C being a constant independent of k and h.

Lemma 2 *Suppose $\boldsymbol{m}_h^{n-1}$ and $\boldsymbol{m}_h^n$ satisfies $|\boldsymbol{m}_l^{n-1}| = |\boldsymbol{m}_l^{n-1}| = 1$ for all $l \in L$ in the equation (2.14). It has a unique solution if $\frac{k}{h^2}$ satisfies*

$$
\frac{k}{h^2} \le 2^{-d-1}. \qquad (2.25)
$$

Proof Suppose V^1 and V^2 are the solution of (2.14), i.e.,

$$
\frac{V_l^i - \boldsymbol{m}_l^{n-1}}{2k} - \alpha \frac{V_l^i + \boldsymbol{m}_l^{n-1}}{2} \times \left(\frac{V_l^i - \boldsymbol{m}_l^{n-1}}{2k} + \frac{2\tau}{k^2}\boldsymbol{m}_l^n \right) = -\frac{1}{h^2}\frac{V_l^i + \boldsymbol{m}_l^{n-1}}{2} \times \left(\sum_{|l-\hat{l}|=1} \frac{V_{l-\hat{l}}^i + \boldsymbol{m}_{l-\hat{l}}^{n-1}}{2} \right) \qquad (2.26)
$$

for $i = 1, 2$. Since $|V_l^i| = 1$ for all $l \in L$, we get the estimate

$$
\| \frac{V^k + \boldsymbol{m}_h}{2} \|_\infty \le 1.
$$

By (2.26), we have

$$
\begin{aligned}
\frac{V_l^1 - V_l^2}{2k} &= -\frac{\alpha}{4k}(V_l^1 - V_l^2) \times \boldsymbol{m}_l^{n-1} + \frac{\alpha\tau}{k^2}(V_l^1 - V_l^2) \times \boldsymbol{m}_l^n - \frac{1}{h^2}\frac{V_l^1 - V_l^2}{2}\\
&\quad \times \left(\sum_{|l-\hat{l}|=1} \frac{V_{l-\hat{l}}^1 + \boldsymbol{m}_{l-\hat{l}}^{n-1}}{2} \right) - \frac{1}{h^2}\frac{V_l^2 + \boldsymbol{m}_l^{n-1}}{2} \times \left(\sum_{|l-\hat{l}|=1} \frac{V_{l-\hat{l}}^1 - V_{l-\hat{l}}^2}{2} \right).
\end{aligned}
$$

The error $\|V^1 - V^2\|_2$ satisfies

$$
\|V^1 - V^2\|_2 \le \frac{2^{d+1}k}{h^2}\|V^1 - V^2\|_2.
$$

Hence, $\|V^1 - V^2\|_2 = 0$ if and only if

$$\frac{k}{h^2} < 2^{-d-1}.$$

This completes the proof.

Remark 1 In the above Lemma, we give a unique solvability in the $\ell^2(\Omega_h)$-norm sense. However, if we consider the norm $\|V^1 - V^2\|_\infty$, we will see that

$$\|V^1 - V^2\|_\infty \leq \left(\frac{\alpha}{2} + \frac{2\alpha\tau}{k} + \frac{2^{d+1}k}{h^2}\right)\|V^1 - V^2\|_\infty. \tag{2.27}$$

This implies that the unique solvability of the scheme (2.14), in the $\ell^\infty(\Omega_h)$ sense, is constrained by $k \leq C_1 h^2$ and $\tau \leq C_2 k$, where C_1 and C_2 are constants independent of h and k.

Meanwhile, it is noticed that, given the initial profile of $\boldsymbol{m}$ at $t = 0$, namely $\boldsymbol{m}^0$, an accurate approximation to $\boldsymbol{m}^1$ and $\boldsymbol{m}^2$ has to be made. In more details, an $O(k^2 + h^2)$ accurate approximation of both $\boldsymbol{m}^1$, $\boldsymbol{m}^2$ and $\frac{\boldsymbol{m}^1-\boldsymbol{m}^0}{k}$, $\frac{\boldsymbol{m}^2-\boldsymbol{m}^1}{k}$ is needed in the convergence analysis.

The initial profile $\boldsymbol{m}^0$ could be taken as $\boldsymbol{m}^0 = \boldsymbol{m}(\cdot, 0)$. This in turn gives a trivial zero initial error for $\boldsymbol{m}^0$. For $\boldsymbol{m}^1$ and $\boldsymbol{m}^2$, a careful Taylor expansion reveals that

$$\begin{aligned}\boldsymbol{m}^1 =&\boldsymbol{m}^0 + k\partial_t \boldsymbol{m}^0 + \frac{k^2}{2}\partial_{tt}\boldsymbol{m}^0 + O(k^3)\\ =&\boldsymbol{m}^0 + \frac{k^2}{2}\partial_{tt}\boldsymbol{m}^0 + O(k^3),\end{aligned} \tag{2.28}$$

$$\begin{aligned}\boldsymbol{m}^2 =&\boldsymbol{m}^0 + 2k\partial_t \boldsymbol{m}^0 + 2k^2\partial_{tt}\boldsymbol{m}^0 + O(k^3)\\ =&\boldsymbol{m}^0 + 2k^2\partial_{tt}\boldsymbol{m}^0 + O(k^3),\end{aligned} \tag{2.29}$$

in which the initial data (2.2c), $\partial_t \boldsymbol{m}(\cdot, 0) \equiv 0$, has been applied in the derivation. Therefore, an accurate approximation to $\boldsymbol{m}^1$ and $\boldsymbol{m}^2$ relies on a precise value of $\partial_{tt}\boldsymbol{m}$ at $t = 0$. An evaluation of the original PDE (2.2a) implies that

$$\boldsymbol{m}^0 \times (\partial_{tt}\boldsymbol{m}^0) = \frac{1}{\alpha\tau}\boldsymbol{m}^0 \times (\Delta \boldsymbol{m}^0 + \mathbf{H}_{\mathrm{e}}^0), \tag{2.30}$$

in which the trivial initial data (2.2c) has been applied again. Meanwhile, motivated by the point-wise temporal differentiation identity

$$\boldsymbol{m} \cdot \partial_{tt}\boldsymbol{m} = -(\partial_t \boldsymbol{m})^2 + \frac{1}{2}\partial_{tt}(|\boldsymbol{m}|^2) = -(\partial_t \boldsymbol{m})^2, \tag{2.31}$$

and the fact that $|\boldsymbol{m}| \equiv 1$, we see that its evaluation at $t = 0$ yields

$$\boldsymbol{m}^0 \cdot \partial_{tt}\boldsymbol{m}^0 = -(\partial_t \boldsymbol{m}^0)^2 = 0. \tag{2.32}$$

Subsequently, a combination of (2.31) and (2.32) uniquely determines $\partial_{tt}\boldsymbol{m}^0$:

$$\partial_{tt}\boldsymbol{m}^0 = -\frac{1}{\alpha\tau}\boldsymbol{m}^0 \times (\boldsymbol{m}^0 \times (\Delta \boldsymbol{m}^0 + \mathbf{H}_{\mathrm{e}}^0)), \tag{2.33}$$

and a substitution of this value into (2.28), (2.29) leads to an $O(k^3)$ approximation to $\boldsymbol{m}^1$ and $\boldsymbol{m}^2$.

Moreover, with spatial approximation introduced, an $O(k^2 + h^2)$ accuracy is obtained for both $\boldsymbol{m}^1$, $\boldsymbol{m}^2$ and $\frac{\boldsymbol{m}^1-\boldsymbol{m}^0}{k}$, $\frac{\boldsymbol{m}^2-\boldsymbol{m}^1}{k}$. This finishes the initialization process.

3 Unconditional Convergence Analysis

The theoretical result concerning the convergence analysis is stated below.

Theorem 2 *Assume that the exact solution of (2.2) has the regularity* $\boldsymbol{m}_e \in C^4([0,T];[C^0(\bar{\Omega})]^3) \cap C^2([0,T];[C^2(\bar{\Omega})]^3) \cap L^\infty([0,T];[C^4(\bar{\Omega})]^3)$. *Denote a nodal interpolation operator* $\mathcal{P}_h$ *such that* $\mathcal{P}_h \boldsymbol{m}_h \in C^1(\Omega)$, *and the numerical solution* $\boldsymbol{m}_h^n$ $(n \geq 0)$ *obtained from (2.13) with the initial error satisfying* $\|\boldsymbol{e}_h^p\|_2 + \|\nabla_h \boldsymbol{e}_h^p\|_2 = \mathcal{O}(k^2+h^2)$, *where* $\boldsymbol{e}_h^p = \mathcal{P}_h \boldsymbol{m}_e(\cdot, t_p) - \boldsymbol{m}_h^p$, $p = 0, 1, 2$, *and* $\|\frac{\boldsymbol{e}_h^{q+1} - \boldsymbol{e}_h^q}{k}\|_2 = \mathcal{O}(k^2+h^2)$, $q = 0, 1$. *Then the following convergence result holds for* $2 \leq n \leq \left\lfloor \frac{T}{k} \right\rfloor$ *as* $h, k \to 0^+$:

$$\|\mathcal{P}_h \boldsymbol{m}_e(\cdot, t_n) - \boldsymbol{m}_h^n\|_2 + \|\nabla_h (\mathcal{P}_h \boldsymbol{m}_e(\cdot, t_n) - \boldsymbol{m}_h^n)\|_2 \leq \mathcal{C}(k^2 + h^2), \tag{3.1}$$

in which the constant $\mathcal{C} > 0$ *is independent of* k *and* h.

Before the rigorous proof is given, the following estimates are declared, which will be utilized in the convergence analysis. In the sequel, for simplicity of notation, we will use a uniform constant $\mathcal{C}$ to denote all the controllable constants throughout this part.

Lemma 3 (Discrete gradient acting on cross product) [10] *For grid functions* $\boldsymbol{f}_h$ *and* $\boldsymbol{g}_h$ *over the uniform numerical grid, we have*

$$\|\nabla_h (\boldsymbol{f}_h \times \boldsymbol{g}_h)\|_2 \leq \mathcal{C}\Big(\|\boldsymbol{f}_h\|_2 \cdot \|\nabla_h \boldsymbol{g}_h\|_\infty + \|\boldsymbol{g}_h\|_\infty \cdot \|\nabla_h \boldsymbol{f}_h\|_2 \Big). \tag{3.2}$$

Lemma 4 (Point-wise product involved with second order temporal stencil) *For grid functions* $\boldsymbol{f}_h$ *and* $\boldsymbol{g}_h$ *over the time domain, we have*

$$\begin{aligned} \frac{\boldsymbol{f}_h^{n+1} - 2\boldsymbol{f}_h^n + \boldsymbol{f}_h^{n-1}}{k^2} \cdot \boldsymbol{g}_h^n &= -\frac{\boldsymbol{f}_h^n - \boldsymbol{f}_h^{n-1}}{k} \cdot \frac{\boldsymbol{g}_h^n - \boldsymbol{g}_h^{n-1}}{k} \\ &\quad + \frac{1}{k}\Big(\frac{\boldsymbol{f}_h^{n+1} - \boldsymbol{f}_h^n}{k} \cdot \boldsymbol{g}_h^n - \frac{\boldsymbol{f}_h^n - \boldsymbol{f}_h^{n-1}}{k} \cdot \boldsymbol{g}_h^{n-1} \Big). \end{aligned} \tag{3.3}$$

Now we proceed into the convergence estimate. First, we construct an approximate solution $\underline{\boldsymbol{m}}$:

$$\underline{\boldsymbol{m}} = \boldsymbol{m}_e + h^2 \boldsymbol{m}^{(1)}, \tag{3.4}$$

in which $\boldsymbol{m}^{(1)}$ is an auxiliary field. To maintain the model consistency, we also need $\Delta \underline{\boldsymbol{m}} = \Delta \boldsymbol{m}_e + h^2 \Delta \boldsymbol{m}^{(1)}$ with $\Delta \boldsymbol{m}^{(1)}$ being bounded uniformly. Hence, the auxiliary field $\boldsymbol{m}^{(1)}$ is set to satisfy the following Poisson equation

$$\begin{aligned} &\Delta \boldsymbol{m}^{(1)} = \hat{C} \quad \text{with} \quad \hat{C} = \frac{1}{|\Omega|} \int_{\partial\Omega} \partial_\nu^3 \boldsymbol{m}_e \, \mathrm{d}s, \\ &\partial_z \boldsymbol{m}^{(1)} \mid_{z=0} = -\frac{1}{24} \partial_z^3 \boldsymbol{m}_e \mid_{z=0}, \quad \partial_z \boldsymbol{m}^{(1)} \mid_{z=1} = \frac{1}{24} \partial_z^3 \boldsymbol{m}_e \mid_{z=1}, \end{aligned} \tag{3.5}$$

with boundary conditions along x and y directions defined in a similar way. The scalar function $\hat{C} = \hat{C}(t)$ is chosen as $\int_\Omega \hat{C} \mathrm{d}\boldsymbol{x} = \int_{\partial\Omega} \partial_\nu \boldsymbol{m}^{(1)} \mathrm{d}\nu$ for maintaining the consistency with the Neumann boundary condition. This class of construction can be found in the related works [26–28]; the purpose of such a construction will be more clearly observed in the later derivation.

Then we extend the approximate profile $\underline{\boldsymbol{m}}$ to the numerical "ghost" points. Applying the extrapolation formula:

$$\underline{\boldsymbol{m}}_{i,j,0} = \underline{\boldsymbol{m}}_{i,j,1}, \quad \underline{\boldsymbol{m}}_{i,j,nz+1} = \underline{\boldsymbol{m}}_{i,j,nz}, \tag{3.6}$$

and the extrapolation for other boundaries can be formulated in the same manner. We will see that such an extrapolation yields a higher order $\mathcal{O}(h^5)$ approximation, instead of the standard $\mathcal{O}(h^3)$ accuracy.

Performing a careful Taylor expansion for the exact solution around the boundary section $z = 0$, combined with the mesh point values: $z_0 = -\frac{1}{2}h$, $z_1 = \frac{1}{2}h$, we get

$$\begin{aligned} \boldsymbol{m}_e(x_i, y_j, z_0) &= \boldsymbol{m}_e(x_i, y_j, z_1) - h\partial_z \boldsymbol{m}_e(x_i, y_j, 0) - \frac{h^3}{24}\partial_z^3 \boldsymbol{m}_e(x_i, y_j, 0) + \mathcal{O}(h^5) \\ &= \boldsymbol{m}_e(x_i, y_j, z_1) - \frac{h^3}{24}\partial_z^3 \boldsymbol{m}_e(x_i, y_j, 0) + \mathcal{O}(h^5), \end{aligned} \tag{3.7}$$

in which the homogenous boundary condition has been applied in the second step. A similar Taylor expansion for the constructed profile $\boldsymbol{m}^{(1)}$ reveals that

$$\begin{aligned} \boldsymbol{m}^{(1)}(x_i, y_j, z_0) &= \boldsymbol{m}^{(1)}(x_i, y_j, z_1) - h\partial_z \boldsymbol{m}^{(1)}(x_i, y_j, 0) + \mathcal{O}(h^3) \\ &= \boldsymbol{m}^{(1)}(x_i, y_j, z_1) + \frac{h}{24}\partial_z^3 \boldsymbol{m}_e(x_i, y_j, 0) + \mathcal{O}(h^3). \end{aligned} \tag{3.8}$$

with the boundary condition in (3.5) applied. In turn, a substitution of (3.7)-(3.8) into (3.4) indicates that

$$\begin{aligned} \underline{\boldsymbol{m}}(x_i, y_j, z_0) &= \boldsymbol{m}_e(x_i, y_j, z_0) + h^2 \boldsymbol{m}^{(1)}(x_i, y_j, z_0) \\ &= \boldsymbol{m}_e(x_i, y_j, z_1) + h^2 \boldsymbol{m}^{(1)}(x_i, y_j, z_1) + \mathcal{O}(h^5), \end{aligned}$$

i.e.,

$$\underline{\boldsymbol{m}}(x_i, y_j, z_0) = \underline{\boldsymbol{m}}(x_i, y_j, z_1) + \mathcal{O}(h^5). \tag{3.9}$$

In other words, the extrapolation formula (3.6) is indeed $\mathcal{O}(h^5)$ accurate.

As a result of the boundary extrapolation estimate (3.9), we see that the discrete Laplacian of $\underline{\boldsymbol{m}}$ yields the second-order accuracy at all the mesh points (including boundary points):

$$\Delta_h \underline{\boldsymbol{m}}_{i,j,k} = \Delta \boldsymbol{m}_e(x_i, y_j, z_k) + \mathcal{O}(h^2), \tag{3.10}$$

for any $0 \le i \le nx+1, 0 \le j \le ny+1, 0 \le k \le nz+1$. In other words, the construction (3.5) ensures an $\mathcal{O}(h^5)$ boundary extrapolation accuracy, as given by (3.9). This in turn leads to a second order spatial accuracy for the discrete Laplacian operator, at both the interior and boundary points.

Moreover, a detailed calculation of Taylor expansion, in both time and space, leads to the following truncation error estimate:

$$\begin{aligned} \frac{\underline{\boldsymbol{m}}_h^{n+1} - \underline{\boldsymbol{m}}_h^{n-1}}{2k} &= \frac{\underline{\boldsymbol{m}}_h^{n+1} + \underline{\boldsymbol{m}}_h^{n-1}}{2} \times \Big(\alpha \frac{\underline{\boldsymbol{m}}_h^{n+1} - \underline{\boldsymbol{m}}_h^{n-1}}{2k} + \\ &\alpha\tau \frac{\underline{\boldsymbol{m}}_h^{n+1} - 2\underline{\boldsymbol{m}}_h^{n} + \underline{\boldsymbol{m}}_h^{n-1}}{k^2} - \Delta_h \Big(\frac{\underline{\boldsymbol{m}}_h^{n+1} + \underline{\boldsymbol{m}}_h^{n-1}}{2}\Big)\Big) + \tau^n, \end{aligned} \tag{3.11}$$

where $\|\tau^n\|_2 \le \mathcal{C}(k^2 + h^2)$. In addition, a higher order Taylor expansion in space and time reveals the following estimate for the discrete gradient of the truncation error, in both time and space:

$$\|\nabla_h \tau^n\|_2, \ \|\frac{\tau^n - \tau^{n-1}}{k}\|_2 \le \mathcal{C}(k^2 + h^2). \tag{3.12}$$

In fact, such a discrete $\|\cdot\|_{H_h^1}$ bound for the truncation comes from the regularity assumption for the exact solution, $\boldsymbol{m}_e \in C^4([0,T];[C^0(\bar{\Omega})]^3) \cap C^2([0,T];[C^2(\bar{\Omega})]^3) \cap L^\infty([0,T];[C^4(\bar{\Omega})]^3)$, as stated in (2.15) and (2.16), as well as the fact that $\boldsymbol{m}^{(1)} \in C^1([0,T];[C^1(\bar{\Omega})]^3) \cap L^\infty([0,T];[C^2(\bar{\Omega})]^3)$, as indicated by the Poisson equation (3.5). Therefore, the regularity of $\underline{\boldsymbol{m}}$ is same as the regularity of $\boldsymbol{m}^{(1)}$, i.e., $\underline{\boldsymbol{m}} \in C^1([0,T];[C^1(\bar{\Omega})]^3) \cap L^\infty([0,T];[C^2(\bar{\Omega})]^3)$.

We introduce the numerical error function $\boldsymbol{e}_h^n = \underline{\boldsymbol{m}}_h^n - \boldsymbol{m}_h^n$, instead of a direct comparison between the numerical solution and the exact solution. The error function between the numerical solution and the constructed solution $\underline{\boldsymbol{m}}_h$ will be analyzed, due to its higher order consistency estimate (3.9) around the boundary. Therefore, a subtraction of (2.14) from the consistency estimate (3.11) leads to the error function evolution system:

$$\frac{\boldsymbol{e}_h^{n+1} - \boldsymbol{e}_h^{n-1}}{2k} = \frac{\boldsymbol{m}_h^{n+1} + \boldsymbol{m}_h^{n-1}}{2} \times \tilde{\boldsymbol{\mu}}_h^n + \frac{\boldsymbol{e}_h^{n+1} + \boldsymbol{e}_h^{n-1}}{2} \times \underline{\boldsymbol{\mu}}_h^n + \tau^n, \tag{3.13}$$

$$\underline{\boldsymbol{\mu}}_h^n := \alpha\Big(\frac{\underline{\boldsymbol{m}}_h^{n+1} - \underline{\boldsymbol{m}}_h^{n-1}}{2k} + \tau\frac{\underline{\boldsymbol{m}}_h^{n+1} - 2\underline{\boldsymbol{m}}_h^n + \underline{\boldsymbol{m}}_h^{n-1}}{k^2}\Big) - \Delta_h\Big(\frac{\underline{\boldsymbol{m}}_h^{n+1} + \underline{\boldsymbol{m}}_h^{n-1}}{2}\Big), \tag{3.14}$$

$$\tilde{\boldsymbol{\mu}}_h^n := \alpha\Big(\frac{\boldsymbol{e}_h^{n+1} - \boldsymbol{e}_h^{n-1}}{2k} + \tau\frac{\boldsymbol{e}_h^{n+1} - 2\boldsymbol{e}_h^n + \boldsymbol{e}_h^{n-1}}{k^2}\Big) - \Delta_h\Big(\frac{\boldsymbol{e}_h^{n+1} + \boldsymbol{e}_h^{n-1}}{2}\Big), \tag{3.15}$$

where τ^n is the truncated error at t_n.

Before proceeding into the formal estimate, we establish a W_h^∞ bound for $\underline{\boldsymbol{\mu}}_h^n$, which is based on the constructed approximate solution $\underline{\boldsymbol{m}}$ (by (3.14)). Since $\underline{\boldsymbol{m}}(\boldsymbol{x},t) = \boldsymbol{m}_e(\boldsymbol{x},t) + h^2\boldsymbol{m}^{(1)}(\boldsymbol{x},t) \in C^1([0,T];[C^1(\bar{\Omega})]^3) \cap L^\infty([0,T];[C^2(\bar{\Omega})]^3)$, we see that the bound $\|\underline{\boldsymbol{\mu}}_h^n\|_\infty$ becomes directly available. Then, there exist constants C_1 and C_2 such that

$$\|\nabla_h \underline{\boldsymbol{\mu}}_h^{n-1}\|_\infty, \|\nabla_h \underline{\boldsymbol{\mu}}_h^n\|_\infty \le C_1, \ \|\frac{\underline{\boldsymbol{\mu}}_h^n - \underline{\boldsymbol{\mu}}_h^{n-1}}{k}\|_\infty \le C_2,$$

where C_1 and C_2 depend on h and k, respectively. For simplicity, we denote

$$\|\underline{\boldsymbol{\mu}}_h^\ell\|_\infty, \ \|\nabla_h \underline{\boldsymbol{\mu}}_h^\ell\|_\infty, \ \|\frac{\underline{\boldsymbol{\mu}}_h^n - \underline{\boldsymbol{\mu}}_h^{n-1}}{k}\|_\infty \le \mathcal{C}, \quad \ell = n, n-1. \tag{3.16}$$

In addition, the following preliminary estimate will be useful in the convergence analysis.

Lemma 5 (A preliminary error estimate) *We have*

$$\|\boldsymbol{e}_h^\ell\|_2^2 \le 2\|\boldsymbol{e}_h^0\|_2^2 + 2Tk\sum_{j=0}^{\ell-1}\Big\|\frac{\boldsymbol{e}_h^{j+1} - \boldsymbol{e}_h^j}{k}\Big\|_2^2, \quad \forall \ell \cdot k \le T. \tag{3.17}$$

Proof We begin with the expansion:

$$\boldsymbol{e}_h^\ell = \boldsymbol{e}_h^0 + k\sum_{j=0}^{\ell-1}\frac{\boldsymbol{e}_h^{j+1} - \boldsymbol{e}_h^j}{k}, \quad \forall \ell \cdot k \le T. \tag{3.18}$$

In turn, a careful application of the Cauchy inequality reveals that

$$\|\boldsymbol{e}_h^\ell\|_2^2 \le 2\Big(\|\boldsymbol{e}_h^0\|_2^2 + k^2\Big\|\sum_{j=0}^{\ell-1}\frac{\boldsymbol{e}_h^{j+1} - \boldsymbol{e}_h^j}{k}\Big\|_2^2\Big), \tag{3.19}$$

$$k^2 \Big\| \sum_{j=0}^{\ell-1} \frac{\boldsymbol{e}_h^{j+1} - \boldsymbol{e}_h^j}{k} \Big\|_2^2 \le k^2 \cdot \ell \cdot \sum_{j=0}^{\ell-1} \Big\| \frac{\boldsymbol{e}_h^{j+1} - \boldsymbol{e}_h^j}{k} \Big\|_2^2 \le Tk \sum_{j=0}^{\ell-1} \Big\| \frac{\boldsymbol{e}_h^{j+1} - \boldsymbol{e}_h^j}{k} \Big\|_2^2, \tag{3.20}$$

in which the fact that $\ell \cdot k \le T$ has been applied. Therefore, a combination of (3.19) and (3.20) yields the desired estimate (3.17). This completes the proof of Lemma 5. □

Taking a discrete inner product with the numerical error equation (3.13) by $\tilde{\boldsymbol{\mu}}_h^n$ gives

$$\begin{aligned} \frac{1}{2k} \langle \boldsymbol{e}_h^{n+1} - \boldsymbol{e}_h^{n-1}, \tilde{\boldsymbol{\mu}}_h^n \rangle =& \langle \frac{\boldsymbol{m}_h^{n+1} + \boldsymbol{m}_h^{n-1}}{2} \times \tilde{\boldsymbol{\mu}}_h^n, \tilde{\boldsymbol{\mu}}_h^n \rangle \\ &+ \langle \frac{\boldsymbol{e}_h^{n+1} + \boldsymbol{e}_h^{n-1}}{2} \times \underline{\boldsymbol{\mu}}_h^n, \tilde{\boldsymbol{\mu}}_h^n \rangle + \langle \tau^n, \tilde{\boldsymbol{\mu}}_h^n \rangle. \end{aligned} \tag{3.21}$$

The analysis on the left hand side of (3.21) is similar to the ones in (2.21)-(2.23):

$$\begin{aligned} \frac{1}{2k} \langle \boldsymbol{e}_h^{n+1} - \boldsymbol{e}_h^{n-1}, \tilde{\boldsymbol{\mu}}_h^n \rangle =& \frac{\alpha\tau}{2k^3} \langle \boldsymbol{e}_h^{n+1} - \boldsymbol{e}_h^{n-1}, \boldsymbol{e}_h^{n+1} - 2\boldsymbol{e}_h^n + \boldsymbol{e}_h^{n-1} \rangle \\ &+ \frac{\alpha}{4k^2} \langle \boldsymbol{e}_h^{n+1} - \boldsymbol{e}_h^{n-1}, \boldsymbol{e}_h^{n+1} - \boldsymbol{e}_h^{n-1} \rangle \\ &+ \frac{1}{4k} \Big\langle \nabla_h (\boldsymbol{e}_h^{n+1} - \boldsymbol{e}_h^{n-1}), \nabla_h (\boldsymbol{e}_h^{n+1} + \boldsymbol{e}_h^{n-1}) \Big\rangle, \end{aligned} \tag{3.22}$$

$$\langle \boldsymbol{e}_h^{n+1} - \boldsymbol{e}_h^{n-1}, \boldsymbol{e}_h^{n+1} - \boldsymbol{e}_h^{n-1} \rangle = \| \boldsymbol{e}^{n+1} - \boldsymbol{e}_h^{n-1} \|_2^2 \ge 0, \tag{3.23}$$

$$\begin{aligned} &\langle \boldsymbol{e}_h^{n+1} - \boldsymbol{e}_h^{n-1}, \boldsymbol{e}_h^{n+1} - 2\boldsymbol{e}_h^n + \boldsymbol{e}_h^{n-1} \rangle \\ &= \| \boldsymbol{e}_h^{n+1} - \boldsymbol{e}_h^n \|_2^2 - \| \boldsymbol{e}_h^n - \boldsymbol{e}_h^{n-1} \|_2^2, \end{aligned} \tag{3.24}$$

$$\begin{aligned} &\Big\langle \boldsymbol{e}_h^{n+1} - \boldsymbol{e}_h^{n-1}, -\Delta_h (\boldsymbol{e}_h^{n+1} + \boldsymbol{e}_h^{n-1}) \Big\rangle \\ &\quad = \Big\langle \nabla_h (\boldsymbol{e}_h^{n+1} - \boldsymbol{e}_h^{n-1}), \nabla_h (\boldsymbol{e}_h^{n+1} + \boldsymbol{e}_h^{n-1}) \Big\rangle = \| \nabla_h \boldsymbol{e}_h^{n+1} \|_2^2 - \| \nabla_h \boldsymbol{e}_h^{n-1} \|_2^2 \\ &\quad = (\| \nabla_h \boldsymbol{e}_h^{n+1} \|_2^2 + \| \nabla_h \boldsymbol{e}_h^n \|_2^2) - (\| \nabla_h \boldsymbol{e}_h^n \|_2^2 + \| \nabla_h \boldsymbol{e}_h^{n-1} \|_2^2). \end{aligned} \tag{3.25}$$

This in turn leads to the following identity:

$$\frac{1}{2k} \langle \boldsymbol{e}_h^{n+1} - \boldsymbol{e}_h^{n-1}, \tilde{\boldsymbol{\mu}}_h^n \rangle = \frac{1}{k} (E_{\boldsymbol{e},h}^{n+1} - E_{\boldsymbol{e},h}^n) + \frac{\alpha}{4k^2} \| \boldsymbol{e}_h^{n+1} - \boldsymbol{e}_h^{n-1} \|_2^2, \tag{3.26}$$

$$E_{\boldsymbol{e},h}^{n+1} = \frac{\alpha\tau}{2} \Big\| \frac{\boldsymbol{e}_h^{n+1} - \boldsymbol{e}_h^n}{k} \Big\|_2^2 + \frac{1}{4} \Big(\| \nabla_h \boldsymbol{e}_h^{n+1} \|_2^2 + \| \nabla_h \boldsymbol{e}_h^n \|_2^2 \Big). \tag{3.27}$$

The first term on the right hand side of (3.21) vanishes, due to the fact that $\frac{\boldsymbol{m}_h^{n+1} + \boldsymbol{m}_h^{n-1}}{2} \times \tilde{\boldsymbol{\mu}}_h^n$ is orthogonal to $\tilde{\boldsymbol{\mu}}_h^n$, at a point-wise level:

$$\langle \frac{\boldsymbol{m}_h^{n+1} + \boldsymbol{m}_h^{n-1}}{2} \times \tilde{\boldsymbol{\mu}}_h^n, \tilde{\boldsymbol{\mu}}_h^n \rangle = 0. \tag{3.28}$$

The second term on the right hand side of (3.21) contains three parts:

$$\langle \frac{\boldsymbol{e}_h^{n+1} + \boldsymbol{e}_h^{n-1}}{2} \times \underline{\boldsymbol{\mu}}_h^n, \tilde{\boldsymbol{\mu}}_h^n \rangle = I_1 + I_2 + I_3, \tag{3.29}$$

$$I_1 = \alpha \langle \frac{\boldsymbol{e}_h^{n+1} + \boldsymbol{e}_h^{n-1}}{2} \times \underline{\boldsymbol{\mu}}_h^n, \frac{\boldsymbol{e}_h^{n+1} - \boldsymbol{e}_h^{n-1}}{2k} \rangle, \tag{3.30}$$

$$I_2 = \alpha\tau \langle \frac{\boldsymbol{e}_h^{n+1} + \boldsymbol{e}_h^{n-1}}{2} \times \underline{\boldsymbol{\mu}}_h^n, \frac{\boldsymbol{e}_h^{n+1} - 2\boldsymbol{e}_h^n + \boldsymbol{e}_h^{n-1}}{k^2} \rangle, \tag{3.31}$$

$$I_3 = \langle \frac{\boldsymbol{e}_h^{n+1} + \boldsymbol{e}_h^{n-1}}{2} \times \underline{\boldsymbol{\mu}}_h^n, -\Delta_h \Big(\frac{\boldsymbol{e}_h^{n+1} + \boldsymbol{e}_h^{n-1}}{2} \Big) \rangle. \tag{3.32}$$

The first inner product, I_1, could be bounded in a straightforward way, with the help of discrete Hölder inequality:

$$\begin{aligned} I_1 =& \alpha \langle \frac{\boldsymbol{e}_h^{n+1} + \boldsymbol{e}_h^{n-1}}{2} \times \underline{\boldsymbol{\mu}}_h^n, \frac{\boldsymbol{e}_h^{n+1} - \boldsymbol{e}_h^{n-1}}{2k} \rangle \\ \le& \frac{\alpha}{4} \| \boldsymbol{e}_h^{n+1} + \boldsymbol{e}_h^{n-1} \|_2 \cdot \| \underline{\boldsymbol{\mu}}_h^n \|_\infty \cdot \Big\| \frac{\boldsymbol{e}_h^{n+1} - \boldsymbol{e}_h^{n-1}}{k} \Big\|_2 \\ \le& \mathcal{C} \| \boldsymbol{e}_h^{n+1} + \boldsymbol{e}_h^{n-1} \|_2 \cdot \Big\| \frac{\boldsymbol{e}_h^{n+1} - \boldsymbol{e}_h^{n-1}}{k} \Big\|_2 \\ \le& \mathcal{C} \left(\| \boldsymbol{e}_h^{n+1} \|_2^2 + \| \boldsymbol{e}_h^{n-1} \|_2^2 + \Big\| \frac{\boldsymbol{e}_h^{n+1} - \boldsymbol{e}_h^{n-1}}{k} \Big\|_2^2 \right). \end{aligned} \tag{3.33}$$

For the second inner product, I_2, we denote $\boldsymbol{g}_h^n := \frac{\boldsymbol{e}_h^{n+1} + \boldsymbol{e}_h^{n-1}}{2} \times \underline{\boldsymbol{\mu}}_h^n$. An application of point-wise identity (3.3) (in Lemma 4) reveals that

$$\begin{aligned} I_2 =& \alpha \tau \langle \boldsymbol{g}_h^n, \frac{\boldsymbol{e}_h^{n+1} - 2\boldsymbol{e}_h^n + \boldsymbol{e}_h^{n-1}}{k^2} \rangle \\ =& -\alpha \tau \langle \frac{\boldsymbol{e}_h^n - \boldsymbol{e}_h^{n-1}}{k}, \frac{\boldsymbol{g}_h^n - \boldsymbol{g}_h^{n-1}}{k} \rangle \\ &+ \frac{\alpha \tau}{k} \Big(\langle \frac{\boldsymbol{e}_h^{n+1} - \boldsymbol{e}_h^n}{k}, \boldsymbol{g}_h^n \rangle - \langle \frac{\boldsymbol{e}_h^n - \boldsymbol{e}_h^{n-1}}{k}, \boldsymbol{g}_h^{n-1} \rangle \Big). \end{aligned} \tag{3.34}$$

Meanwhile, the following expansion is observed:

$$\begin{aligned} \frac{\boldsymbol{g}_h^n - \boldsymbol{g}_h^{n-1}}{k} =& \frac{1}{4} \Big(\frac{\boldsymbol{e}_h^{n+1} - \boldsymbol{e}_h^n}{k} + \frac{\boldsymbol{e}_h^{n-1} - \boldsymbol{e}_h^{n-2}}{k} \Big) \times (\underline{\boldsymbol{\mu}}_h^n + \underline{\boldsymbol{\mu}}_h^{n-1}) \\ &+ \frac{\boldsymbol{e}_h^{n+1} + \boldsymbol{e}_h^n + \boldsymbol{e}_h^{n-1} + \boldsymbol{e}_h^{n-2}}{4} \times \frac{\underline{\boldsymbol{\mu}}_h^n - \underline{\boldsymbol{\mu}}_h^{n-1}}{k}. \end{aligned} \tag{3.35}$$

This in turn indicates the associated estimate:

$$\begin{aligned} \Big\| \frac{\boldsymbol{g}_h^n - \boldsymbol{g}_h^{n-1}}{k} \Big\|_2 \le& \frac{1}{4} \Big(\Big\| \frac{\boldsymbol{e}_h^{n+1} - \boldsymbol{e}_h^n}{k} \|_2 + \Big\| \frac{\boldsymbol{e}_h^{n-1} - \boldsymbol{e}_h^{n-2}}{k} \Big\|_2 \Big) \cdot (\| \underline{\boldsymbol{\mu}}_h^n \|_\infty + \| \underline{\boldsymbol{\mu}}_h^{n-1} \|_\infty) \\ &+ \frac{\| \boldsymbol{e}_h^{n+1} \|_2 + \| \boldsymbol{e}_h^n \|_2 + \| \boldsymbol{e}_h^{n-1} \|_2 + \| \boldsymbol{e}_h^{n-2} \|_2}{4} \cdot \Big\| \frac{\underline{\boldsymbol{\mu}}_h^n - \underline{\boldsymbol{\mu}}_h^{n-1}}{k} \Big\|_\infty \\ \le& \mathcal{C} \Big(\Big\| \frac{\boldsymbol{e}_h^{n+1} - \boldsymbol{e}_h^n}{k} \Big\|_2 + \Big\| \frac{\boldsymbol{e}_h^{n-1} - \boldsymbol{e}_h^{n-2}}{k} \Big\|_2 \\ &+ \| \boldsymbol{e}_h^{n+1} \|_2 + \| \boldsymbol{e}_h^n \|_2 + \| \boldsymbol{e}_h^{n-1} \|_2 + \| \boldsymbol{e}_h^{n-2} \|_2 \Big), \end{aligned} \tag{3.36}$$

in which the bound (3.16) has been applied. Going back to (3.34), we see that

$$\begin{aligned} -\alpha \tau \langle \frac{\boldsymbol{e}_h^n - \boldsymbol{e}_h^{n-1}}{k}, \frac{\boldsymbol{g}_h^n - \boldsymbol{g}_h^{n-1}}{k} \rangle \le& \alpha \tau \Big\| \frac{\boldsymbol{e}_h^n - \boldsymbol{e}_h^{n-1}}{k} \Big\|_2 \cdot \Big\| \frac{\boldsymbol{g}_h^n - \boldsymbol{g}_h^{n-1}}{k} \Big\|_2 \\ \le& \mathcal{C} \Big(\Big\| \frac{\boldsymbol{e}_h^{n+1} - \boldsymbol{e}_h^n}{k} \Big\|_2 + \Big\| \frac{\boldsymbol{e}_h^{n-1} - \boldsymbol{e}_h^{n-2}}{k} \Big\|_2 + \| \boldsymbol{e}_h^{n+1} \|_2 \end{aligned}$$

$$+ \|\boldsymbol{e}_h^n\|_2 + \|\boldsymbol{e}_h^{n-1}\|_2 + \|\boldsymbol{e}_h^{n-2}\|_2\Big) \Big\| \frac{\boldsymbol{e}_h^n - \boldsymbol{e}_h^{n-1}}{k} \Big\|_2$$
$$\le \mathcal{C}\Big(\Big\| \frac{\boldsymbol{e}_h^{n+1} - \boldsymbol{e}_h^n}{k} \Big\|_2^2 + \Big\| \frac{\boldsymbol{e}_h^{n-1} - \boldsymbol{e}_h^{n-2}}{k} \Big\|_2^2 + \|\boldsymbol{e}_h^{n+1}\|_2^2$$
$$+ \|\boldsymbol{e}_h^n\|_2^2 + \|\boldsymbol{e}_h^{n-1}\|_2^2 + \|\boldsymbol{e}_h^{n-2}\|_2^2 + \Big\| \frac{\boldsymbol{e}_h^n - \boldsymbol{e}_h^{n-1}}{k} \Big\|_2^2 \Big), \tag{3.37}$$

Hence, we get the estimate

$$\begin{aligned} I_2 \le& \mathcal{C}\Big(\Big\| \frac{\boldsymbol{e}_h^{n+1} - \boldsymbol{e}_h^n}{k} \Big\|_2^2 + \Big\| \frac{\boldsymbol{e}_h^{n-1} - \boldsymbol{e}_h^{n-2}}{k} \Big\|_2^2 + \|\boldsymbol{e}_h^{n+1}\|_2^2 \\ &+ \|\boldsymbol{e}_h^n\|_2^2 + \|\boldsymbol{e}_h^{n-1}\|_2^2 + \|\boldsymbol{e}_h^{n-2}\|_2^2 + \Big\| \frac{\boldsymbol{e}_h^n - \boldsymbol{e}_h^{n-1}}{k} \Big\|_2^2 \Big) \\ &+ \frac{\alpha\tau}{k}\Big(\langle \frac{\boldsymbol{e}_h^{n+1} - \boldsymbol{e}_h^n}{k}, \boldsymbol{g}_h^n \rangle - \langle \frac{\boldsymbol{e}_h^n - \boldsymbol{e}_h^{n-1}}{k}, \boldsymbol{g}_h^{n-1} \rangle \Big). \end{aligned} \tag{3.38}$$

For the third inner product part, I_3, an application of summation by parts formula gives

$$\begin{aligned} I_3 =& \langle \frac{\boldsymbol{e}_h^{n+1} + \boldsymbol{e}_h^{n-1}}{2} \times \underline{\boldsymbol{\mu}}_h^n, -\Delta_h \Big(\frac{\boldsymbol{e}_h^{n+1} + \boldsymbol{e}_h^{n-1}}{2} \Big) \rangle \\ =& \langle \nabla_h \Big(\frac{\boldsymbol{e}_h^{n+1} + \boldsymbol{e}_h^{n-1}}{2} \times \underline{\boldsymbol{\mu}}_h^n \Big), \nabla_h \Big(\frac{\boldsymbol{e}_h^{n+1} + \boldsymbol{e}_h^{n-1}}{2} \Big) \rangle. \end{aligned} \tag{3.39}$$

Meanwhile, we make use of the preliminary inequality (3.2) (in Lemma 3) and get

$$\begin{aligned} &\Big\| \nabla_h \Big(\frac{\boldsymbol{e}_h^{n+1} + \boldsymbol{e}_h^{n-1}}{2} \times \underline{\boldsymbol{\mu}}_h^n \Big) \Big\|_2 \\ &\le \mathcal{C}\Big(\Big\| \frac{\boldsymbol{e}_h^{n+1} + \boldsymbol{e}_h^{n-1}}{2} \Big\|_2 \cdot \|\nabla_h \underline{\boldsymbol{\mu}}_h^n\|_\infty + \|\underline{\boldsymbol{\mu}}_h^n\|_\infty \cdot \Big\| \nabla_h \Big(\frac{\boldsymbol{e}_h^{n+1} + \boldsymbol{e}_h^{n-1}}{2}) \Big\|_2 \Big) \\ &\le \mathcal{C}\Big(\Big\| \frac{\boldsymbol{e}_h^{n+1} + \boldsymbol{e}_h^{n-1}}{2} \Big\|_2 + \Big\| \nabla_h \Big(\frac{\boldsymbol{e}_h^{n+1} + \boldsymbol{e}_h^{n-1}}{2} \Big) \Big\|_2 \Big) \\ &\le \mathcal{C}\Big(\|\boldsymbol{e}_h^{n+1}\|_2 + \|\boldsymbol{e}_h^{n-1}\|_2 + \|\nabla_h \boldsymbol{e}_h^{n+1}\|_2 + \|\nabla_h \boldsymbol{e}_h^{n-1}\|_2 \Big). \end{aligned} \tag{3.40}$$

Again, the bound (3.16) has been applied in the derivation. Therefore, the following estimate is available for I_3:

$$\begin{aligned} I_3 \le& \Big\| \nabla_h \Big(\frac{\boldsymbol{e}_h^{n+1} + \boldsymbol{e}_h^{n-1}}{2} \times \underline{\boldsymbol{\mu}}_h^n \Big) \Big\|_2 \cdot \Big\| \nabla_h \Big(\frac{\boldsymbol{e}_h^{n+1} + \boldsymbol{e}_h^{n-1}}{2} \Big) \Big\|_2 \\ \le& \mathcal{C}\Big(\|\boldsymbol{e}_h^{n+1}\|_2 + \|\boldsymbol{e}_h^{n-1}\|_2 + \|\nabla_h \boldsymbol{e}_h^{n+1}\|_2 + \|\nabla_h \boldsymbol{e}_h^{n-1}\|_2 \Big) \\ &\cdot \Big(\|\nabla_h \boldsymbol{e}_h^{n+1}\|_2 + \|\nabla_h \boldsymbol{e}_h^{n-1}\|_2 \Big) \\ \le& \mathcal{C}\Big(\|\boldsymbol{e}_h^{n+1}\|_2^2 + \|\boldsymbol{e}_h^{n-1}\|_2^2 + \|\nabla_h \boldsymbol{e}_h^{n+1}\|_2^2 + \|\nabla_h \boldsymbol{e}_h^{n-1}\|_2^2 \Big). \end{aligned} \tag{3.41}$$

The estimate of I_3 can also be obtained by a direct application of discrete Hölder inequality:

$$\begin{aligned} I_3 =& \langle \Big(\frac{\boldsymbol{e}_h^{n+1} + \boldsymbol{e}_h^{n-1}}{2} \times \nabla_h \underline{\boldsymbol{\mu}}_h^n \Big), \nabla_h \Big(\frac{\boldsymbol{e}_h^{n+1} + \boldsymbol{e}_h^{n-1}}{2} \Big) \rangle \\ \le& \frac{1}{4} \|\boldsymbol{e}_h^{n+1} + \boldsymbol{e}_h^{n-1}\|_2 \cdot \|\nabla_h \underline{\boldsymbol{\mu}}_h^n\|_\infty \cdot \|\nabla_h (\boldsymbol{e}_h^{n+1} + \boldsymbol{e}_h^{n-1})\|_2 \end{aligned}$$

$$\leq \mathcal{C}\Big(\|e_h^{n+1}\|_2^2 + \|e_h^{n-1}\|_2^2 + \|\nabla_h e_h^{n+1}\|_2^2 + \|\nabla_h e_h^{n-1}\|_2^2\Big). \tag{3.42}$$

A substitution of (3.33), (3.38) and (3.42) into (3.29) yields the following bound:

$$\begin{aligned}
&\langle \frac{e_h^{n+1}+e_h^{n-1}}{2} \times \underline{\mu}_h^n, \tilde{\mu}_h^n\rangle = I_1 + I_2 + I_3 \\
&\leq \mathcal{C}\Big(\Big\|\frac{e_h^{n+1}-e_h^n}{k}\Big\|_2^2 + \Big\|\frac{e_h^n-e_h^{n-1}}{k}\Big\|_2^2 + \Big\|\frac{e_h^{n-1}-e_h^{n-2}}{k}\Big\|_2^2 \\
&\quad + \|e_h^{n+1}\|_2^2 + \|e_h^n\|_2^2 + \|e_h^{n-1}\|_2^2 + \|e_h^{n-2}\|_2^2 + \|\nabla_h e_h^{n+1}\|_2^2 + \|\nabla_h e_h^{n-1}\|_2^2\Big) \\
&\quad + \frac{\alpha\tau}{k}\Big(\langle \frac{e_h^{n+1}-e_h^n}{k}, g_h^n\rangle - \langle \frac{e_h^n-e_h^{n-1}}{k}, g_h^{n-1}\rangle\Big).
\end{aligned} \tag{3.43}$$

The third term on the right hand side of (3.21) could be analyzed in a similar fashion:

$$\langle \tau^n, \tilde{\mu}_h^n\rangle = I_4 + I_5 + I_6, \tag{3.44}$$

$$I_4 = \alpha\langle \tau^n, \frac{e_h^{n+1}-e_h^{n-1}}{2k}\rangle, \quad I_5 = \alpha\tau\langle \tau^n, \frac{e_h^{n+1}-2e_h^n+e_h^{n-1}}{k^2}\rangle, \tag{3.45}$$

$$I_6 = \langle \tau^n, -\Delta_h\Big(\frac{e_h^{n+1}+e_h^{n-1}}{2}\Big)\rangle. \tag{3.46}$$

By the direct calculation, we have

$$\begin{aligned}
I_4 =& \alpha\langle \tau^n, \frac{e_h^{n+1}-e_h^{n-1}}{2k}\rangle \leq \frac{\alpha}{2}\|\tau^n\|_2 \cdot \Big\|\frac{e_h^{n+1}-e_h^{n-1}}{k}\Big\|_2 \\
\leq& \frac{\alpha}{4}\left(\|\tau^n\|_2^2 + \Big\|\frac{e_h^{n+1}-e_h^{n-1}}{k}\Big\|_2^2\right),
\end{aligned} \tag{3.47}$$

and

$$I_5 = -\alpha\tau\langle \frac{e_h^n-e_h^{n-1}}{k}, \frac{\tau^n-\tau^{n-1}}{k}\rangle + \frac{\alpha\tau}{k}\Big(\langle \frac{e_h^{n+1}-e_h^n}{k}, \tau^n\rangle - \langle \frac{e_h^n-e_h^{n-1}}{k}, \tau^{n-1}\rangle\Big), \tag{3.48}$$

in which

$$\begin{aligned}
&-\langle \frac{e_h^n-e_h^{n-1}}{k}, \frac{\tau^n-\tau^{n-1}}{k}\rangle \leq \Big\|\frac{e_h^n-e_h^{n-1}}{k}\Big\|_2 \cdot \Big\|\frac{\tau^n-\tau^{n-1}}{k}\Big\|_2 \\
&\leq \mathcal{C}(k^2+h^2)\Big\|\frac{e_h^n-e_h^{n-1}}{k}\Big\|_2 \leq \mathcal{C}(k^4+h^4) + \frac{1}{2}\Big\|\frac{e_h^n-e_h^{n-1}}{k}\Big\|_2^2.
\end{aligned} \tag{3.49}$$

We therefore get the bound for I_5:

$$\begin{aligned}
I_5 \leq& \mathcal{C}(k^4+h^4) + \frac{\alpha\tau}{2}\Big\|\frac{e_h^n-e_h^{n-1}}{k}\Big\|_2^2 \\
&+ \frac{\alpha\tau}{k}\Big(\langle \frac{e_h^{n+1}-e_h^n}{k}, \tau^n\rangle - \langle \frac{e_h^n-e_h^{n-1}}{k}, \tau^{n-1}\rangle\Big).
\end{aligned} \tag{3.50}$$

Next, for I_6 we have

$$I_6 = \langle \tau^n, -\Delta_h\Big(\frac{e_h^{n+1}+e_h^{n-1}}{2}\Big)\rangle = \langle \nabla_h\tau^n, \nabla_h\Big(\frac{e_h^{n+1}+e_h^{n-1}}{2}\Big)\rangle$$

$$
\begin{aligned}
&\le \|\nabla_h \tau^n\|_2 \cdot \Big\| \nabla_h \Big(\frac{\boldsymbol{e}_h^{n+1} + \boldsymbol{e}_h^{n-1}}{2} \Big) \Big\|_2 \le \mathcal{C}(k^2 + h^2) \Big\| \nabla_h \Big(\frac{\boldsymbol{e}_h^{n+1} + \boldsymbol{e}_h^{n-1}}{2} \Big) \Big\|_2 \\
&\le \mathcal{C}(k^4 + h^4) + \frac{1}{2} \Big(\|\nabla_h \boldsymbol{e}_h^{n+1}\|_2^2 + \|\nabla_h \boldsymbol{e}_h^{n-1}\|_2^2 \Big).
\end{aligned} \tag{3.51}
$$

Notice that the truncation error estimate (3.12) has been repeatedly applied in the above derivation. Going back to (3.44), we obtain

$$
\begin{aligned}
\langle \tau^n, \tilde{\boldsymbol{\mu}}_h^n \rangle \le & \mathcal{C}(k^4 + h^4) + \frac{\alpha}{2} \Big\| \frac{\boldsymbol{e}_h^{n+1} - \boldsymbol{e}_h^n}{k} \Big\|_2^2 + \frac{\alpha(\tau+1)}{2} \Big\| \frac{\boldsymbol{e}_h^n - \boldsymbol{e}_h^{n-1}}{k} \Big\|_2^2 \\
& + \frac{1}{2} \Big(\|\nabla_h \boldsymbol{e}_h^{n+1}\|_2^2 + \|\nabla_h \boldsymbol{e}_h^{n-1}\|_2^2 \Big) \\
& + \frac{\alpha\tau}{k} \Big(\langle \frac{\boldsymbol{e}_h^{n+1} - \boldsymbol{e}_h^n}{k}, \tau^n \rangle - \langle \frac{\boldsymbol{e}_h^n - \boldsymbol{e}_h^{n-1}}{k}, \tau^{n-1} \rangle \Big).
\end{aligned} \tag{3.52}
$$

Finally, a substitution of (3.26), (3.27), (3.28), (3.43) and (3.52) into (3.21) leads to the following inequality:

$$
\begin{aligned}
& \frac{1}{k}(E_{\boldsymbol{e},h}^{n+1} - E_{\boldsymbol{e},h}^n) + \frac{\alpha}{4k^2} \|\boldsymbol{e}_h^{n+1} - \boldsymbol{e}_h^{n-1}\|_2^2 \\
& \le \mathcal{C}(k^4 + h^4) + \mathcal{C} \Big(\Big\| \frac{\boldsymbol{e}_h^{n+1} - \boldsymbol{e}_h^n}{k} \Big\|_2^2 + \Big\| \frac{\boldsymbol{e}_h^n - \boldsymbol{e}_h^{n-1}}{k} \Big\|_2^2 + \Big\| \frac{\boldsymbol{e}_h^{n-1} - \boldsymbol{e}_h^{n-2}}{k} \Big\|_2^2 \\
& \quad + \|\boldsymbol{e}_h^{n+1}\|_2^2 + \|\boldsymbol{e}_h^n\|_2^2 + \|\boldsymbol{e}_h^{n-1}\|_2^2 + \|\boldsymbol{e}_h^{n-2}\|_2^2 + \|\nabla_h \boldsymbol{e}_h^{n+1}\|_2^2 + \|\nabla_h \boldsymbol{e}_h^{n-1}\|_2^2 \Big) \\
& \quad + \frac{\alpha\tau}{k} \Big(\langle \frac{\boldsymbol{e}_h^{n+1} - \boldsymbol{e}_h^n}{k}, \boldsymbol{g}_h^n + \tau^n \rangle - \langle \frac{\boldsymbol{e}_h^n - \boldsymbol{e}_h^{n-1}}{k}, \boldsymbol{g}_h^{n-1} + \tau^{n-1} \rangle \Big).
\end{aligned} \tag{3.53}
$$

Subsequently, a summation in time yields

$$
\begin{aligned}
E_{\boldsymbol{e},h}^{n+1} \le & E_{\boldsymbol{e},h}^2 + \mathcal{C}T(k^4 + h^4) + \mathcal{C}k \Big(\sum_{j=0}^{n} \Big\| \frac{\boldsymbol{e}_h^{j+1} - \boldsymbol{e}_h^j}{k} \Big\|_2^2 + \sum_{j=0}^{n+1} (\|\boldsymbol{e}_h^j\|_2^2 + \|\nabla_h \boldsymbol{e}_h^j\|_2^2) \Big) \\
& + \alpha\tau \Big(\langle \frac{\boldsymbol{e}_h^{n+1} - \boldsymbol{e}_h^n}{k}, \boldsymbol{g}_h^n + \tau^n \rangle - \langle \frac{\boldsymbol{e}_h^2 - \boldsymbol{e}_h^1}{k}, \boldsymbol{g}_h^1 + \tau^1 \rangle \Big).
\end{aligned} \tag{3.54}
$$

For the term $\alpha\tau\langle \frac{\boldsymbol{e}_h^{n+1} - \boldsymbol{e}_h^n}{k}, \boldsymbol{g}_h^n + \tau^n \rangle$, the following estimate could be derived

$$
\alpha\tau \langle \frac{\boldsymbol{e}_h^{n+1} - \boldsymbol{e}_h^n}{k}, \boldsymbol{g}_h^n + \tau^n \rangle \le \frac{\alpha\tau}{4} \Big\| \frac{\boldsymbol{e}_h^{n+1} - \boldsymbol{e}_h^n}{k} \Big\|_2^2 + 2\alpha\tau(\|\boldsymbol{g}_h^n\|_2^2 + \|\tau^n\|_2^2), \tag{3.55}
$$

$$
\begin{aligned}
\|\boldsymbol{g}_h^n\|_2 = & \Big\| \frac{\boldsymbol{e}_h^{n+1} + \boldsymbol{e}_h^{n-1}}{2} \times \underline{\boldsymbol{\mu}}_h^n \Big\|_2 \le \Big\| \frac{\boldsymbol{e}_h^{n+1} + \boldsymbol{e}_h^{n-1}}{2} \Big\|_2 \cdot \|\underline{\boldsymbol{\mu}}_h^n\|_\infty \\
& \le \mathcal{C} \Big\| \frac{\boldsymbol{e}_h^{n+1} + \boldsymbol{e}_h^{n-1}}{2} \Big\|_2 \le \mathcal{C}(\|\boldsymbol{e}_h^{n+1}\|_2 + \|\boldsymbol{e}_h^{n-1}\|_2),
\end{aligned} \tag{3.56}
$$

in which the bound (3.16) has been used again. Then we get

$$
\begin{aligned}
\alpha\tau \langle \frac{\boldsymbol{e}_h^{n+1} - \boldsymbol{e}_h^n}{k}, \boldsymbol{g}_h^n + \tau^n \rangle \le & \frac{\alpha\tau}{4} \Big\| \frac{\boldsymbol{e}_h^{n+1} - \boldsymbol{e}_h^n}{k} \Big\|_2^2 + 2\alpha\tau\|\tau^n\|_2^2 \\
& + \mathcal{C}(\|\boldsymbol{e}_h^{n+1}\|_2^2 + \|\boldsymbol{e}_h^{n-1}\|_2^2) \\
\le & \frac{1}{2} E_{\boldsymbol{e},h}^{n+1} + 2\alpha\tau\|\tau^n\|_2^2 + \mathcal{C}(\|\boldsymbol{e}_h^{n+1}\|_2^2 + \|\boldsymbol{e}_h^{n-1}\|_2^2),
\end{aligned} \tag{3.57}
$$

in which the expansion identity, $E_{\boldsymbol{e},h}^{n+1} = \frac{\alpha\tau}{2}\|\frac{\boldsymbol{e}_h^{n+1}-\boldsymbol{e}_h^n}{k}\|_2^2 + \frac{1}{4}(\|\nabla_h \boldsymbol{e}_h^{n+1}\|_2^2 + \|\nabla_h \boldsymbol{e}_h^n\|_2^2)$ (given by (3.27)), has been applied. Its substitution into (3.54) gives

$$E_{\boldsymbol{e},h}^{n+1} \leq 2E_{\boldsymbol{e},h}^2 + \mathcal{C}T(k^4+h^4) + \mathcal{C}k\Big(\sum_{j=0}^{n}\Big\|\frac{\boldsymbol{e}_h^{j+1}-\boldsymbol{e}_h^j}{k}\Big\|_2^2 + \sum_{j=0}^{n+1}(\|\boldsymbol{e}_h^j\|_2^2 + \|\nabla_h \boldsymbol{e}_h^j\|_2^2)\Big)$$
$$+ \mathcal{C}(\|\boldsymbol{e}_h^{n+1}\|_2^2 + \|\boldsymbol{e}_h^{n-1}\|_2^2) + 4\alpha\tau\|\tau^n\|_2^2 - 2\alpha\tau\langle\frac{\boldsymbol{e}_h^2-\boldsymbol{e}_h^1}{k}, \boldsymbol{g}_h^1 + \tau^1\rangle. \tag{3.58}$$

Moreover, an application of the preliminary error estimate (3.17) (in Lemma 5) leads to

$$E_{\boldsymbol{e},h}^{n+1} \leq 2E_{\boldsymbol{e},h}^2 + \mathcal{C}T(k^4+h^4) + \mathcal{C}(T^2+1)k\sum_{j=0}^{n}\Big\|\frac{\boldsymbol{e}_h^{j+1}-\boldsymbol{e}_h^j}{k}\Big\|_2^2 + \mathcal{C}T\|\boldsymbol{e}_h^0\|_2^2$$
$$+ \mathcal{C}k\sum_{j=0}^{n+1}\|\nabla_h \boldsymbol{e}_h^j\|_2^2 + 4\alpha\tau\|\tau^n\|_2^2 - 2\alpha\tau\langle\frac{\boldsymbol{e}_h^2-\boldsymbol{e}_h^1}{k}, \boldsymbol{g}_h^1 + \tau^1\rangle, \tag{3.59}$$

in which we have made use of the following fact:

$$k\sum_{j=0}^{n+1}\|\boldsymbol{e}_h^j\|_2^2 \leq k\cdot(n+1)\Big(2\|\boldsymbol{e}_h^0\|_2^2 + 2Tk\sum_{j=0}^{n}\Big\|\frac{\boldsymbol{e}_h^{j+1}-\boldsymbol{e}_h^j}{k}\Big\|_2^2\Big)$$
$$\leq 2T\|\boldsymbol{e}_h^0\|_2^2 + 2T^2k\sum_{j=0}^{n}\Big\|\frac{\boldsymbol{e}_h^{j+1}-\boldsymbol{e}_h^j}{k}\Big\|_2^2. \tag{3.60}$$

In addition, for the initial error quantities, the following estimates are available:

$$E_{\boldsymbol{e},h}^2 = \frac{\alpha\tau}{2}\Big\|\frac{\boldsymbol{e}_h^2-\boldsymbol{e}_h^1}{k}\Big\|_2^2 + \frac{1}{4}\left(\|\nabla_h \boldsymbol{e}_h^2\|_2^2 + \|\nabla_h \boldsymbol{e}_h^1\|_2^2\right) \leq \mathcal{C}\left(k^4+h^4\right), \tag{3.61}$$
$$\|\boldsymbol{e}_h^0\|_2^2 \leq \mathcal{C}\left(k^4+h^4\right), \tag{3.62}$$
$$4\alpha\tau\|\tau^n\|_2^2 \leq \mathcal{C}\left(k^4+h^4\right), \tag{3.63}$$
$$\|\boldsymbol{g}_h^1\|_2 = \Big\|\frac{\boldsymbol{e}_h^2+\boldsymbol{e}_h^0}{2}\times\underline{\boldsymbol{\mu}}_h^1\Big\|_2 \leq \Big\|\frac{\boldsymbol{e}_h^2+\boldsymbol{e}_h^0}{2}\Big\|_2\cdot\|\underline{\boldsymbol{\mu}}_h^1\|_\infty \leq \mathcal{C}\left(k^2+h^2\right), \tag{3.64}$$
$$-2\alpha\tau\langle\frac{\boldsymbol{e}_h^2-\boldsymbol{e}_h^1}{k}, \boldsymbol{g}_h^1+\tau^1\rangle \leq 2\alpha\tau\Big\|\frac{\boldsymbol{e}_h^2-\boldsymbol{e}_h^1}{k}\Big\|_2\cdot\left(\|\boldsymbol{g}_h^1\|_2 + \|\tau^1\|_2\right)$$
$$\leq \mathcal{C}\left(k^4+h^4\right), \tag{3.65}$$

which comes from the assumption in Theorem 2. Then we arrive at

$$E_{\boldsymbol{e},h}^{n+1} \leq \mathcal{C}\left(T^2+1\right)k\sum_{j=0}^{n}\Big\|\frac{\boldsymbol{e}_h^{j+1}-\boldsymbol{e}_h^j}{k}\Big\|_2^2 + \mathcal{C}k\sum_{j=0}^{n+1}\|\nabla_h \boldsymbol{e}_h^j\|_2^2 + \mathcal{C}(T+1)\left(k^4+h^4\right)$$
$$\leq \mathcal{C}(T+1)\left(k^4+h^4\right) + \mathcal{C}\left(T^2+1\right)k\sum_{j=0}^{n}E_{\boldsymbol{e},h}^{j+1}, \tag{3.66}$$

in which the fact that $E_{\boldsymbol{e},h}^{j+1} = \frac{\alpha\tau}{2}\|\frac{\boldsymbol{e}_h^{j+1}-\boldsymbol{e}_h^j}{k}\|_2^2 + \frac{1}{4}(\|\nabla_h \boldsymbol{e}_h^{j+1}\|_2^2 + \|\nabla_h \boldsymbol{e}_h^j\|_2^2)$, has been used. In turn, an application of discrete Gronwall inequality results in the desired convergence estimate:

$$E_{\boldsymbol{e},h}^{n+1} \le \mathcal{C}Te^{\mathcal{C}T}\left(k^4+h^4\right), \quad \text{for all } (n+1): n+1 \le \left\lfloor \frac{T}{k} \right\rfloor, \tag{3.67}$$

$$\left\| \frac{\boldsymbol{e}_h^{n+1}-\boldsymbol{e}_h^n}{k} \right\|_2 + \|\nabla_h \boldsymbol{e}_h^{n+1}\|_2 \le \mathcal{C}\left(k^2+h^2\right). \tag{3.68}$$

Again, an application of the preliminary error estimate (3.17) (in Lemma 5) implies that

$$\|\boldsymbol{e}_h^{n+1}\|_2^2 \le 2\|\boldsymbol{e}_h^0\|_2^2 + 2Tk\sum_{j=0}^{n}\left\| \frac{\boldsymbol{e}_h^{j+1}-\boldsymbol{e}_h^j}{k} \right\|_2^2 \le \mathcal{C}\left(k^4+h^4\right), \tag{3.69}$$

A combination of (3.68) and (3.69) finishes the proof of Theorem 2.

4 A Numerical Solver for the Nonlinear System

It is clear that Algorithm 1 is a nonlinear scheme. The following fixed-point iteration is employed to solve it.

Algorithm 2 *Set* $\boldsymbol{m}_h^{n+1,0} = 2\boldsymbol{m}_h^n - \boldsymbol{m}_h^{n-1}$ *and* $p = 0$.

(i) *Compute* $\boldsymbol{m}_h^{n+1,p+1}$ *such that*

$$\begin{aligned}\frac{\boldsymbol{m}_h^{n+1,p+1}-\boldsymbol{m}_h^{n-1}}{2k} &= -\frac{\boldsymbol{m}_h^{n+1,p+1}+\boldsymbol{m}_h^{n-1}}{2}\times\Delta_h\left(\frac{\boldsymbol{m}_h^{n+1,p}+\boldsymbol{m}_h^{n-1}}{2}\right)\\ &+\alpha\frac{\boldsymbol{m}_h^{n+1,p+1}+\boldsymbol{m}_h^{n-1}}{2}\times\left(\frac{\boldsymbol{m}_h^{n+1,p+1}-\boldsymbol{m}_h^{n-1}}{2k}+\tau\frac{\boldsymbol{m}_h^{n+1,p+1}-2\boldsymbol{m}_h^n+\boldsymbol{m}_h^{n-1}}{k^2}\right).\end{aligned} \tag{4.1}$$

(ii) *If* $\|\boldsymbol{m}_h^{n+1,p+1}-\boldsymbol{m}_h^{n+1,p}\|_2 \le \epsilon$, *then stop and set* $\boldsymbol{m}_h^{n+1} = \boldsymbol{m}_h^{n+1,p+1}$.
(iii) *Set* $p \leftarrow p+1$ *and go to* (i).

Denote the operator

$$\mathcal{L}^p = I - \alpha\boldsymbol{m}_h^{n-1}\times - \frac{2\alpha\tau}{k}\boldsymbol{m}_h^n\times - \frac{k}{2}\Delta_h\left(\boldsymbol{m}_h^{n+1,p}+\boldsymbol{m}_h^{n-1}\right)\times, \tag{4.2}$$

and make the fixed-point iteration solve the following equation

$$\mathcal{L}^p\boldsymbol{m}_h^{n+1,p+1} = \boldsymbol{m}_h^{n-1} + \frac{2\alpha\tau}{k}\boldsymbol{m}_h^n\times\boldsymbol{m}_h^{n-1} - \frac{k}{2}\boldsymbol{m}_h^{n-1}\times\Delta_h\left(\boldsymbol{m}_h^{n+1,p}+\boldsymbol{m}_h^{n-1}\right), \tag{4.3}$$

in its inner iteration. Under the condition $k \le Ch^2$ with C a constant, the following lemma confirms the convergence of Algorithm 2. For any $l \in L$ and owing to the property of $|\boldsymbol{m}_h(\boldsymbol{x}_l)| = 1$, it is clear that $0 < \|\boldsymbol{m}_h\|_\infty \le 1$. For the discretized ℓ^2 norm of $\boldsymbol{m}_h$, we have

$$\|\nabla_h\boldsymbol{m}_h\|_2 \le 2h^{-1}\|\boldsymbol{m}_h\|_2. \tag{4.4}$$

Then

$$\begin{aligned}\|\Delta_h\boldsymbol{m}_h\|_2^2 &= -\langle\nabla_h\boldsymbol{m}_h, \nabla_h\Delta_h\boldsymbol{m}_h\rangle\\ &\le \|\nabla_h\boldsymbol{m}_h\|_2\|\nabla_h\Delta_h\boldsymbol{m}_h\|_2 \le 2h^{-1}\|\nabla_h\boldsymbol{m}_h\|_2\|\Delta_h\boldsymbol{m}_h\|_2,\end{aligned} \tag{4.5}$$

which in turn implies the following inverse inequality:

$$\|\Delta_h \boldsymbol{m}_h\|_2 \leq 4h^{-2}\|\boldsymbol{m}_h\|_2. \tag{4.6}$$

Lemma 6 *Let $|\boldsymbol{m}_h^{n-1}| = |\boldsymbol{m}_h^n| = 1$, there exists a constant c_0 such that $\|\boldsymbol{m}_h^{n-1}\|_\infty$, $\|\boldsymbol{m}_h^n\|_\infty \leq c_0$. The solution $\boldsymbol{m}_h^{n+1,p}$ calculated by (4.1) satisfies $|\boldsymbol{m}_h^{n+1,p}| = |\boldsymbol{m}_h^{n-1}|$ for $p = 1, 2, \cdots$, which means that we can still find the constant $c_0 \leq 1$ satisfying $\|\boldsymbol{m}_h^{n+1,p}\|_\infty \leq c_0$. Then, for all $p \geq 1$, there exists a unique solution $\boldsymbol{m}_h^{n+1,p}$ of (4.1) and the following inequality is valid:*

$$\|\boldsymbol{m}_h^{n+1,p+1} - \boldsymbol{m}_h^{n+1,p}\|_2 \leq 4c_0kh^{-2}\|\boldsymbol{m}^{n+1,p} - \boldsymbol{m}^{n+1,p-1}\|_2. \tag{4.7}$$

Proof For any $\boldsymbol{m}_h \in \mathbb{S}^2$, the following identity is clear:

$$\langle \boldsymbol{m}_h, \mathcal{L}^p \boldsymbol{m}_h \rangle = 1,$$

for all $p \geq 1$. Thus the operator $\mathcal{L}^p$ is positive definite for all $p \geq 1$, which provides the unique solvability of (4.1).

Taking the discrete inner product with (4.1) by $\boldsymbol{m}_h^{n+1,p+1} + \boldsymbol{m}_h^{n-1}$, we have $|\boldsymbol{m}_h^{n+1,p+1}| = 1$ in a point-wise sense, which means that the length of the magnetization is preserved at each step in the inner iteration. Thus, we can find a constant $c_0 \leq 1$ to control the ℓ^∞ norm of $\boldsymbol{m}_h^{n-1}$, $\boldsymbol{m}_h^n$ and $\boldsymbol{m}_h^{n+1,p}$ for $p = 1, 2, \cdots$ simultaneously.

Subtraction of two subsequent equations in the fixed-point iteration yields

$$\begin{aligned}
\frac{1}{2k}\left(\boldsymbol{m}_h^{n+1,p+1} - \boldsymbol{m}_h^{n+1,p}\right) = &-\frac{1}{4}\left(\boldsymbol{m}_h^{n+1,p+1} - \boldsymbol{m}_h^{n+1,p}\right) \times \Delta_h \boldsymbol{m}_h^{n+1,p} \\
&-\frac{1}{4}\boldsymbol{m}_h^{n+1,p} \times \Delta_h \left(\boldsymbol{m}_h^{n+1,p} - \boldsymbol{m}_h^{n+1,p-1}\right) \\
&-\frac{1}{4}\boldsymbol{m}_h^{n} \times \Delta_h \left(\boldsymbol{m}^{n+1,p} - \boldsymbol{m}^{n+1,p-1}\right) \\
&-\frac{1}{4}\left(\boldsymbol{m}_h^{n+1,p+1} - \boldsymbol{m}^{n+1,p}\right) \times \Delta_h \boldsymbol{m}_h^{n-1} \\
&+\frac{\alpha}{2k}\boldsymbol{m}_h^{n-1} \times \left(\boldsymbol{m}_h^{n+1,p+1} - \boldsymbol{m}_h^{n+1,p}\right) \\
&+\frac{\alpha\tau}{2k^2}\boldsymbol{m}_h^{n} \times \left(\boldsymbol{m}_h^{n+1,p+1} - \boldsymbol{m}_h^{n+1,p}\right).
\end{aligned}$$

Taking the inner product with $(\boldsymbol{m}_h^{n+1,p+1} - \boldsymbol{m}_h^{n+1,p})$ by the above equation produces

$$\begin{aligned}
\|\boldsymbol{m}_h^{n+1,p+1} - \boldsymbol{m}_h^{n+1,p}\|_2 \leq &\frac{k}{2}\|\boldsymbol{m}_h^{n+1,p}\|_\infty \|\Delta_h \left(\boldsymbol{m}_h^{n+1,p} - \boldsymbol{m}_h^{n+1,p-1}\right)\|_2 \\
&+ \frac{k}{2}\|\boldsymbol{m}_h^{n}\|_\infty \|\Delta_h \left(\boldsymbol{m}_h^{n+1,p} - \boldsymbol{m}_h^{n+1,p-1}\right)\|_2 \\
\leq &c_0 k \|\Delta_h \left(\boldsymbol{m}^{n+1,p} - \boldsymbol{m}^{n+1,p-1}\right)\|_2.
\end{aligned}$$

In turn, the convergence result becomes

$$\|\boldsymbol{m}_h^{n+1,p+1} - \boldsymbol{m}_h^{n+1,p}\|_2 \leq 4c_0kh^{-2}\|\boldsymbol{m}_h^{n+1,p} - \boldsymbol{m}_h^{n+1,p-1}\|_2, \tag{4.8}$$

which completes the proof of Lemma 6.

Table 1 The discrete ℓ^2 and ℓ^∞ errors in terms of the temporal step-size. The spatial mesh-size is fixed as $h = 0.001$ over $\Omega = (0, 1)$ and the final time is $T = 0.01$

k	$\|\boldsymbol{m}_h - \boldsymbol{m}_e\|_2$	$\|\boldsymbol{m}_h - \boldsymbol{m}_e\|_\infty$
T/40	1.2500e−11	1.2584e−11
T/60	5.6887e−12	5.6024e−12
T/80	3.2008e−12	3.1525e−12
T/100	2.0487e−12	2.0174e−12
order	1.97	2.00

Table 2 The discrete ℓ^2 and ℓ^∞ error in terms of the spatial mesh-size. The parameters are set as: the temporal step-size $k = 2.0\text{e}{-}06$, $\Omega = (0, 1)$ and the final time $T = 0.5$

h	$\|\boldsymbol{m}_h - \boldsymbol{m}_e\|_2$	$\|\boldsymbol{m}_h - \boldsymbol{m}_e\|_\infty$
1/20	1.9742e−05	2.5320e−05
1/40	4.9846e−06	6.3459e−06
1/60	2.2340e−06	2.8201e−06
1/80	1.2720e−06	1.5853e−06
order	1.98	2.00

5 Numerical Experiments

5.1 Accuracy Tests

Consider the 1-D iLLG equation with a force term $\mathbf{f}$,

$$\partial_t \boldsymbol{m} = -\boldsymbol{m} \times \partial_{xx}\boldsymbol{m} + \alpha \boldsymbol{m} \times (\partial_t \boldsymbol{m} + \tau \partial_{tt}\boldsymbol{m}) + \mathbf{f}.$$

The exact solution is chosen to be $\boldsymbol{m}_\mathrm{e} = (\cos(\bar{x})\sin(t^2), \sin(\bar{x})\sin(t^2), \cos(t^2))^T$ with $\bar{x} = x^2(1-x)^2$, and the forcing term is given by $\mathbf{f} = \partial_t \boldsymbol{m}_\mathrm{e} + \boldsymbol{m}_\mathrm{e} \times \partial_{xx}\boldsymbol{m}_\mathrm{e} - \alpha \boldsymbol{m}_\mathrm{e} \times (\partial_t \boldsymbol{m}_\mathrm{e} + \tau \partial_{tt}\boldsymbol{m}_\mathrm{e})$. Fixing the tolerance $\epsilon = 1.0\text{e}{-}07$ for the fixed-point iteration, we record the discrete ℓ^2 and ℓ^∞ errors between the exact solution and numerical solution with a sequence of temporal step-size and spatial mesh-size. The parameters in the above 1-D equation are set as: $\alpha = 0.1$, $\tau = 10.0$, and the final time $T = 0.01$. The temporal step-sizes and spatial mesh-sizes are listed in the Tables 1 and 2.

In addition, the 3-D iLLG equation is also considered,

$$\partial_t \boldsymbol{m} = -\boldsymbol{m} \times \Delta \boldsymbol{m} + \alpha \boldsymbol{m} \times (\partial_t \boldsymbol{m} + \tau \partial_{tt}\boldsymbol{m}) + \mathbf{f}.$$

The exact solution is chosen to be $\boldsymbol{m}_\mathrm{e} = (\cos(\bar{x}\bar{y}\bar{z})\sin(t^2), \sin(\bar{x}\bar{y}\bar{z})\sin(t^2)), \cos(t^2))^T$ with $\bar{y} = y^2(1-y)^2$ and $\bar{z} = z^2(1-z)^2$, and the forcing term $\mathbf{f} = \partial_t \boldsymbol{m}_\mathrm{e} + \boldsymbol{m}_\mathrm{e} \times \Delta \boldsymbol{m}_\mathrm{e} - \alpha \boldsymbol{m}_\mathrm{e} \times (\partial_t \boldsymbol{m}_\mathrm{e} + \tau \partial_{tt}\boldsymbol{m}_\mathrm{e})$. Similarly, we record the discrete ℓ^2 and ℓ^∞ errors between exact and numerical solutions as temporal step-size and spatial mesh-size varies. The corresponding parameters are set as: $\alpha = 0.01$ and $\tau = 1000.0$. Besides, the final time of this simulation is $T = 0.01$, with the temporal step-size and spatial mesh-size listed in Tables 3 and 4.

5.2 Micromagnetics Tests

The inertial effect can be observed during the relaxation of a system with a non-equilibrium initialization. To visualize this, we conduct micromagnetics simulations for both the LLG equation and the iLLG equation.

Table 3 The discrete ℓ^2 and ℓ^∞ errors in terms of the temporal step-size. The spatial mesh-size is fixed as $h = 0.001$ and final time is $T = 0.01$

k	$\|\boldsymbol{m}_h - \boldsymbol{m}_e\|_2$	$\|\boldsymbol{m}_h - \boldsymbol{m}_e\|_\infty$
T/100	1.2678e−05	1.2765e−05
T/120	8.8067e−06	8.8830e−06
T/140	6.4725e−06	6.5419e−06
T/160	4.9576e−06	5.0224e−06
order	2.00	1.98

Table 4 The discrete ℓ^2 and ℓ^∞ errors in terms of spatial mesh-size. The temporal step-size is fixed as $k = 2.0\text{e}{-06}$

h	$\|\boldsymbol{m}_h - \boldsymbol{m}_e\|_2$	$\|\boldsymbol{m}_h - \boldsymbol{m}_e\|_\infty$
1/8	1.4392e−07	3.4940e−07
1/10	9.6832e−08	2.2864e−07
1/12	6.9825e−08	1.6079e−07
1/14	5.2828e−08	1.1895e−07
order	1.79	1.92

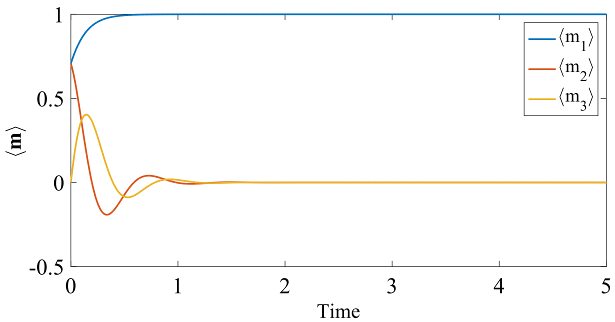

Fig. 1 The relaxation of the spatially averaged magnetization controlled by the LLG equation. The final time is $T = 5.0$ with $k = 0.001$, and the damping parameter is $\alpha = 0.5$

In the following simulations, a 3-D domain $\Omega = [0, 1] \times [0, 1] \times [0, 0.4]$ is uniformly discretized into $10 \times 10 \times 4$ cells, with uniform initialization $\boldsymbol{m}^0 = (\sqrt{2}/2, \sqrt{2}/2, 0)^T$. For comparison, the LLG equation is discretized by the mid-point scheme proposed in [5] with the fixed-point iteration solver proposed in this work. The damping parameter is $\alpha = 0.5$ and the field is fixed as $\mathbf{H}_{\mathrm{e}} = (10, 0, 0)^T$, which indicates that the system shall converge to $\boldsymbol{m} = (1, 0, 0)^T$. Here the relaxation of the magnetization behavior controlled by the LLG equation is visualized in Fig. 1.

As for the counterpart of the LLG equation, wtih a given reference field $\mathbf{H}_{\mathrm{e}}$, the discrete energy of the iLLG equation becomes

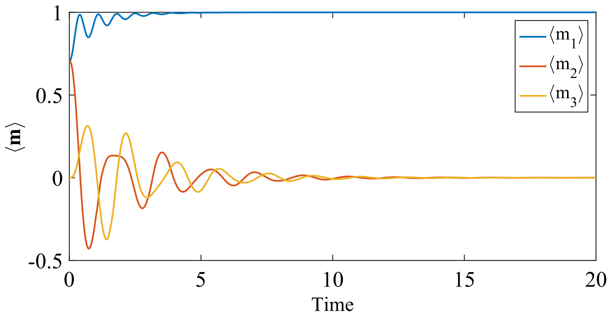

(a) Spatially averaged magnetization

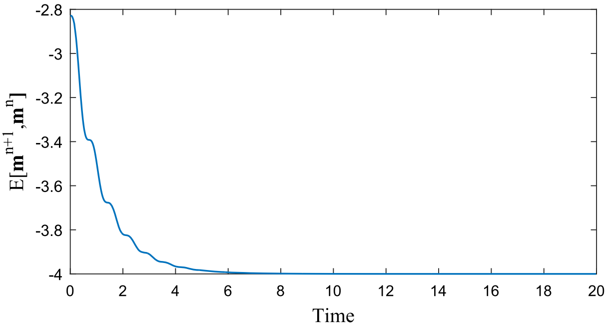

(b) Energy decay

Fig. 2 The spatially averaged magnetization evolution **a** and the energy evolution **b** controlled by the iLLG equation. Parameters settings: $T = 20$, $k = 0.02$, $\tau = 1.0$ and $\alpha = 0.5$

$$
\begin{aligned}
\mathbf{E}[\boldsymbol{m}^{n+1}, \boldsymbol{m}^{n}] &= \frac{1}{4}\left(\|\nabla_h \boldsymbol{m}_h^{n+1}\|_2^2 + \|\nabla_h \boldsymbol{m}_h^{n}\|_2^2\right) \\
&\quad + \frac{\alpha\tau}{2}\left\|\frac{\boldsymbol{m}_h^{n+1} - \boldsymbol{m}_h^{n}}{k}\right\|_2^2 - \frac{1}{2}\langle \boldsymbol{m}_h^{n+1} + \boldsymbol{m}_h^{n}, \mathbf{H}_{\mathrm{e}}\rangle. \qquad (5.1)
\end{aligned}
$$

Setting the inertial parameter $\tau = 1.0$, the spatially averaged magnetization is recorded to depict the inertial effect in Fig. 2a. Meanwhile, the energy decay is also verified as in Fig. 2b. The inertial effect is observed at shorter timescales for magnetization dynamics during the relaxation of the system with a non-equilibrium initialization.

Furthermore, the inertial effect also can be activated by an external perturbation applied to an equilibrium state. Here we set the damping parameter $\alpha = 0.02$ and $\tau = 0.5$, then the time step-size must be reduced to 0.001 with $T = 3.0$. For the equilibrium state $\boldsymbol{m}^0 = (1, 0, 0)^T$, the perturbation $4.0 \times \sin(2\pi f t)$ is applied along y direction over the time interval $[0, 0.05]$, with $f = 20$. The relaxation of the iLLG equation, revealed by the evolution of the spatially averaged magnetization, is visualized in Fig. 3.

6 Conclusion

In this work, we have proposed an implicit mid-point scheme with three time steps to solve the inertial Landau–Lifshitz–Gilbert equation. The energy decay of the system and con-

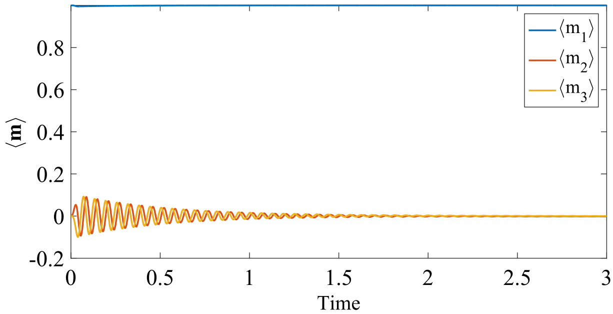

Fig. 3 The response of the spatially averaged magnetization for the magnetic perturbation in the presence of the inertial effect. For the equilibrium initialization $\boldsymbol{m}^0 = (1, 0, 0)^T$, a perturbation $4.0 \times \sin(2\pi f t)$ is applied along y direction during time interval $[0, 0.05]$ with $f = 20$. The basic simulation parameters are: $\alpha = 0.02$, $\tau = 0.5$, $T = 3.0$ and $k = 0.001$

stant length of magnetization in a point wise sense are preserved by the proposed method. By introducing a constructed solution $\underline{\boldsymbol{m}}$ with second order accuracy, we have proved the unconditional convergence in $H^1(\Omega_T)$-norm sense. Due to the inherit nonlinearity, a fix-point iteration solver is required to the numerical scheme. For the theoretical analysis, although the convergence analysis is unconditional, a constraint $k \le Ch^2$ is required for unique solvability and the fix-point iteration solver. In addition, we provide a series of numerical experiments to confirm the theoretical analysis, as well as to observe the nutation of magnetization induced by the inertial effect in micromagnetics simulations.

Funding This work is supported in part by the grant NSFC 11971021 (J. Chen), the program of China Scholarships Council No. 202106920036 (P. Li).

Data Availability Enquiries about data availability should be directed to the authors.

Declarations

Conflict of interest The authors have not disclosed any Conflict of interest.

References

1. Alouges, F.: A new finite element scheme for Landau–Lifchitz equations. Discrete Contin. Dyn. Syst. Ser. S **1**(2), 187–196 (2008)
2. Alouges, F., Jaisson, P.: Convergence of a finite element discretization for the Landau–Lifshitz equations in micromagnetism. Math. Models Methods Appl. Sci. **16**(02), 299–316 (2006)
3. Alouges, F., Kritsikis, E., Toussaint, J.: A convergent finite element approximation for Landau–Lifschitz–Gilbert equation. Phys. B: Condens. Matter **407**(9), 1345–1349 (2012)
4. An, R., Gao, H., Sun, W.: Optimal error analysis of Euler and Crank-Nicolson projection finite difference schemes for Landau–Lifshitz equation. SIAM J. Numer. Anal. **59**(3), 1639–1662 (2021)
5. Bartels, S., Prohl, A.: Convergence of an implicit finite element method for the Landau-Lifshitz–Gilbert equation. SIAM J. Numer. Anal. **44**(4), 1405–1419 (2006)
6. Beaurepaire, E., Merle, J.-C., Daunois, A., Bigot, J.-Y.: Ultrafast spin dynamics in ferromagnetic nickel. Phys. Rev. Lett. **76**, 4250–4253 (1996)
7. Bhattacharjee, S., Nordström, L., Fransson, J.: Atomistic spin dynamic method with both damping and moment of inertia effects included from first principles. Phys. Rev. Lett. **108**, 057204 (2012)

8. Cai, Y., Chen, J., Wang, C., Xie, C.: A second-order numerical method for Landau–Lifshitz–Gilbert equation with large damping parameters. J. Comput. Phys. **451**, 110831 (2022)
9. Cai, Y., Chen, J., Wang, C., Xie, C.: Error analysis of a linear numerical scheme for the Landau–Lifshitz equation with large damping parameters. Math. Methods Apply. Sci. **46**, 18952–18974 (2023)
10. Chen, J., Wang, C., Xie, C.: Convergence analysis of a second-order semi-implicit projection method for Landau–Lifshitz equation. Appl. Numer. Math. **168**, 55–74 (2021)
11. Cimrák, I.: Error estimates for a semi-implicit numerical scheme solving the Landau–Lifshitz equation with an exchange field. IMA J. Numer. Anal. **25**(3), 611–634 (2005)
12. Cimrák, I.: A survey on the numerics and computations for the Landau–Lifshitz equation of micromagnetism. Arch. Comput. Methods Eng. **15**, 277–309 (2008)
13. Ciornei, M.-C., Rubí, J.M., Wegrowe, J.-E.: Magnetization dynamics in the inertial regime: nutation predicted at short time scales. Phys. Rev. B **83**, 020410 (2011)
14. E, W., Wang, X.: Numerical methods for the Landau–Lifshitz equation. SIAM J. Numer. Anal. **38**(5), 1647–1665 (2000)
15. Fähnle, M., Steiauf, D., Illg, C.: Generalized Gilbert equation including inertial damping: derivation from an extended breathing Fermi surface model. Phys. Rev. B **84**, 172403 (2011)
16. Gao, H.: Optimal error estimates of a linearized backward Euler FEM for the Landau–Lifshitz equation. SIAM J. Numer. Anal. **52**(5), 2574–2593 (2014)
17. Gilbert, T.: A Lagrangian formulation of gyromagnetic equation of the magnetization field. Phys. Rev. **100**, 1243–1255 (1955)
18. Kammerer, M., Weigand, M., Curcic, M., Noske, M., Sproll, M., Vansteenkiste, A., Van Waeyenberge, B., Stoll, H., Woltersdorf, G., Back, C.H., Schuetz, G.: Magnetic vortex core reversal by excitation of spin waves. Nat. Commun. **2**, 279 (2011)
19. Koopmans, B., Malinowski, G., Dalla Longa, F., Steiauf, D., Fähnle, M., Roth, T., Cinchetti, M., Aeschlimann, M.: Explaining the paradoxical diversity of ultrafast laser-induced demagnetization. Nat. Mater. **9**, 259–265 (2010)
20. Kritsikis, E., Vaysset, A., Buda-Prejbeanu, L.D., Alouges, F., Toussaint, J.-C.: Beyond first-order finite element schemes in micromagnetics. J. Comput. Phys. **256**, 357–366 (2014)
21. Kružík, M., Prohl, A.: Recent developments in the modeling, analysis, and numerics of ferromagnetism. SIAM Rev. **48**(3), 439–483 (2006)
22. Landau, L., Lifshitz, E.: On the theory of the dispersion of magetic permeability in ferromagnetic bodies. Phys. Z. Sowjetunion **8**, 153–169 (1935)
23. Li, P., Xie, C., Du, R., Chen, J., Wang, X.: Two improved Gauss-Seidel projection methods for Landau–Lifshitz–Gilbert equation. J. Comput. Phys. **401**, 109046 (2020)
24. Li, P., Yang, L., Lan, J., Du, R., Chen, J.: A second-order semi-implicit method for the inertial Landau–Lifshitz–Gilbert equation. Numer. Math. Theor. Meth. Appl. **16**, 182–203 (2023)
25. Romeo, A., Finocchio, G., Carpentieri, M., Torres, L., Consolo, G., Azzerboni, B.: A numerical solution of the magnetization reversal modeling in a permalloy thin film using fifth order Runge–Kutta method with adaptive step size control. Phys. B: Condens. Matter **403**(2), 464–468 (2008)
26. Samelson, R., Temam, R., Wang, C., Wang, S.: Surface pressure poisson equation formulation of the primitive equations: numerical schemes. SIAM J. Numer. Anal. **41**, 1163–1194 (2003)
27. Wang, C., Liu, J.-G.: Convergence of gauge method for incompressible flow. Math. Comp. **69**, 1385–1407 (2000)
28. Wang, C., Liu, J.-G., Johnston, H.: Analysis of a fourth order finite difference method for incompressible Boussinesq equation. Numer. Math. **97**, 555–594 (2004)
29. Wang, X., García-Cervera, C.J., E, W.: A Gauss–Seidel projection method for micromagnetics simulations. J. Comput. Phys. **171**(1), 357–372 (2001)
30. Xie, C., Garciá-Cervera, C.J., Wang, C., Zhou, Z., Chen, J.: Second-order semi-implicit projection methods for micromagnetics simulations. J. Comput. Phys. **404**, 109104 (2020)